Expression and functional analysis of *pthrp1* and *ihha* in the regeneration of bones in zebrafish caudal fin

Ali AL-REWASHDY

Thesis submitted to the Faculty of Graduate and Postdoctoral Studies in partial fulfillment of the requirements for the degree of

Master of Science

In Biology

2013

Department of Biology

Faculty of Science

University of Ottawa

TABLE OF CONTENTS

LIST OF FIGURES

LIST OF ABBREVIATIONS

ACs- articular chondrocytes

BMPs- bone morphogenic proteins

Ci- *cubitus interruptus*

evx1- zebrafish *even-skipped* related gene

DEPC- diethylpyrocarbonate

dpa- days post amputation

dpf- days post fertilization

dpi- days post injection

FGFs- fibroblast growth factors

FPCs- flat proliferative chondrocytes

HCs- hypertrophic chondrocytes

Hh- hedgehog signaling

hpa- hours post amputation

IHH- Indian hedgehog

MO- morpholino

PBS- phosphate buffered saline

PFA- paraformaldehyde

PreHCs- prehypertrophic chondrocytes

Ptc- patched

PTHrP- Parathyroid hormone related protein

RPCs- round proliferative chondrocytes

runx2a- Runt-related transcription factor 2a

SHH- sonic hedgehog

Smo- smoothened

Nomenclature Convention

This is a brief description of the nomenclature convention that will be used in this thesis. I will use the indian hedgehog (IHH) gene as my sample gene for this description. In mammals, human genes, cDNAs and mRNAs would be written as *IHH* and mice genes would be written as *Ihh*. For the proteins, the mammalian convention is IHH for both humans and mice. In zebrafish the convention is the same for genes (and cDNAs or mRNAs) and proteins, except it is non-italic and the first letter is uppercase in proteins. Therefore, the zebrafish gene would be written as *ihh* and the protein would be written as Ihh.

Abstract

The parathyroid hormone related protein (PTHrP) and Indian Hedgehog (IHH) are two secreted molecules, acting as paracrine factors during embryonic development and post-natal growth of endochondral bones. PTHrP and IHH are essential factors for the regulation of chondrocyte proliferation and differentiation. However, it has previously been shown that PTHrP and IHH are also expressed in the chick and mouse embryos intramembranous bones, which do not form through a cartilage intermediate and in which chondrocytes are absent. Similarly, the zebrafish orthologs, *pthrp1* and *ihha,* are also expressed during the regeneration of the intramembranous bones of the fin rays of the zebrafish caudal fin. This surprising observation led us to further analyze the expression and function of *pthrp1* and *ihha* in the regenerating fin rays. Gene expression analysis using *in situ* hybridization shows that *pthrp1* is expressed in a stripe of cells located within the domain of expression of *ihha* in the newly differentiating osteoblasts in the regenerating fin rays. Also, *pthrp1* expression is observed at the level of the joints between the bone segments forming the rays and co-localizes with the expression domain of *evx1,* a transcription factor that has been implicated in the formation of joints in the caudal fin. Furthermore, RT-PCR analyses show that *pthrp2* and the *pthrp receptors* mRNA (*pth1r, pth2r and pth3r*) are also present in the fin regenerate. Finally, functional analysis shows that the knockdown of *pthrp1* or *ihha* expression by electroporation of morpholinos induces a delay of the regenerative outgrowth of the fin. These results suggest that *pthrp1* and *ihha* may be involved in the regulation of proliferation and differentiation of chondrocyte-like osteoblasts in the fin rays, playing a role similar to that described in the mammalian growth plate of endochondral bones. In addition, *pthrp1* is possibly an important factor involved in the formation and maintenance of joints of the dermal bones of the fin rays.

Acknowledgments

I would like to thank my supervisor Dr. Marie-Andree Akimenko for giving me the chance to take part in this project and for all her help and support throughout. I also would like to thank Jing Zhang for the many hours of help she offered to everyone in the lab. Thanks to all my previous and current lab members for offering endless help and support and making every day worthwhile. Thanks to my advisory committee for their helpful information. Special thanks to my family for their continuous love and support. Thanks to my dear friends Shahram Eisa-Beygi, Kevin Lin and Saud Ayed for their help, support and all the beautiful moments we had together.

1. Introduction

1.1 Overview of regeneration

Regeneration is an event that can be found in certain organisms and this event allows for the partial or complete replacement of lost tissue/organs. Depending on the circumstances, regeneration can occur following injury, acting as a mechanism for repair, or it can occur as a constitutive event involved in maintaining the physiological integrity of the organism. There are two types of tissue/organ regeneration: morphallaxis and epimorphosis. In morphallaxis regeneration, such as the type of regeneration occurring in hydra, there is structural and cellular remodeling of the remaining unaffected part of the tissue/organ without an initial involvement of any cell proliferation. In epimorphic regeneration such as during zebrafish fin regeneration and newt limb regeneration, the process involves the formation of a blastema and cell proliferation (Morgan, 1901). The capacity for regeneration has been shown in many non-vertebrate species such as planarian and hydra. However, the incidence of this event is fairly rare in adult vertebrates. Many of the rare incidence of regeneration observed in tetrapods are limited to a specific stage of their life cycle, especially during embryonic development (Han et al., 2005; Yokoyama, 2008). However, teleost fish, such as zebrafish, *Danio rerio*, have an excellent capacity for regeneration throughout their life cycle. Zebrafish are capable of regenerating injured tissues/organs such as heart, liver, brain, retina, to name a few (Tu and Chi 2012).

As stated above, the capacity for regeneration can be found in early development for organisms like mammals and it is absent in the adult stage of life. Examples of this can be seen in embryonic mice being able to regenerate digits (Reginelli et al., 1995; Han et al., 2003). Also, human children

have the ability to regenerate fingertips whereas this capacity is lost in adults (Vidal and Dickson, 1993; Han et al., 2005). When comparing these phenomena with the regenerative capacity of other vertebrates like zebrafish, it leaves one wondering why this capacity was lost in mammals?

1.2 The zebrafish model organism

Zebrafish (*Danio rerio*) is a small freshwater teleost fish of the cyprinid family that belongs to the class of actinopterygii, the ray finned fish. The zebrafish has a well-established repertoire of characteristics for being a valuable organism to study developmental biology and also as a model for human disease (Jung et al., 2012, Tu and Chi, 2012). In addition, there are multiple characteristics that make zebrafish very useful as a model organism for the study of molecular mechanisms of signaling pathways in development and regeneration. Some of the advantages of using zebrafish include the fact that they have a short generation time of about three months and they are highly fertile (each pair can lay 100 to 200 eggs per day). Zebrafish do not require large amounts of space for storage and their maintenance cost is fairly low. Another key advantage is the fact that fertilization is external and the embryos undergo fast and synchronized development (Stainier, 2001). The embryos are also transparent and can be easily imaged *in vivo* using a dissecting microscope.

Multiple tools have been developed for research using the zebrafish model. Reverse genetic approaches include the use of antisense morpholinos, to temporarily knock down gene functions and TILLING and TALEN (Wienholds et al., 2003; Huang et al., 2011) to introduce mutations in a gene of interest. The Sanger institute undertook sequencing of the zebrafish genome and annotated sequences are available on Ensembl (http://www.ensembl.org/Danio_rerio/Info/Index).

A more complete annotation was performed in collaboration with the ZebraFish Information Network (ZFIN) and can be accessed on the World Wide Web through the Vegadatabase (http://vega.sanger.ac.uk/Danio_rerio/index.html). In addition, methods have been developed to allow for the generation of stable transgenic lines, expressing fluorescent reporters under the control of tissue specific promoters (Brittijin et al., 2009).

1.2.1 Zebrafish caudal fin regeneration

Zebrafish have five sets of fins which are divided into two paired fins: pectoral and pelvic fins and three unpaired fins: dorsal, anal and caudal fins (Figure 1.1A). The pectoral and pelvic fins are considered to be homologous to tetrapod paired limbs (Zhang et al., 2010). When studying regeneration, the caudal fin has been employed as one of the excellent organs in zebrafish to perform experimental studies. This is mainly due to its large size and accessibility which permits manipulations (Akimenko et al., 2003, Poss et al., 2003, Schebesta et al., 2006). For example, the fins can be amputated multiple times, each time followed by complete fin regeneration and fin amputation does not impede the animal's life (Azevedo et al., 2011). Due to the bilobed nature of the caudal fin, choosing a control for some experiments is easy because one lobe can be used as such. This is very useful because the control lobe is within the same system and can be considered to act almost in the same fashion as the other lobe. Finally, the caudal fin tissue is relatively thin and transparent making it a great tool for the use of fluorescent reporter transgenic lines.

The skeleton of the caudal fin is composed of a proximal endoskeleton and a distal exoskeleton. The endoskeleton is made of endochondral bone and the exoskeleton is made of intramembranous or dermal bone (Cubbage and Mabee, 1996, Spoorendonk et al., 2010). The exoskeleton is composed of the dermal bony fin rays called lepidotrichia and they are connected to the proximal

endoskeleton by ligaments (Figure 1.1B). When observing a single lepidotrichium, it is composed of two concave hemirays that are facing each other (Figure 1.1C). These hemirays enclose a loose, vascularized and innervated connective tissue, which is surrounded by a multilayered epithelium. The hemirays that make up the lepidotrichia consist of many successive segments that are added through development and regeneration to ensure the longitudinal growth of the hemirays (Akimenko et al., 2003). This growth happens throughout life by distal addition of segments to each ray.

In the caudal fin, one can find 18 fin rays (lepidotrichia) and they form several bifurcations as the fin grows. However, the two most lateral rays do not form any bifurcations. At the distal tip of each lepidotrichia, there are clusters of small rigid fibrils known as actinotrichia. These actinotrichia are un-mineralized structures made of elastoidin, composed of collagen and actinodin, and they extend distally as straight, unbranched spicules (Zhang et al., 2010).

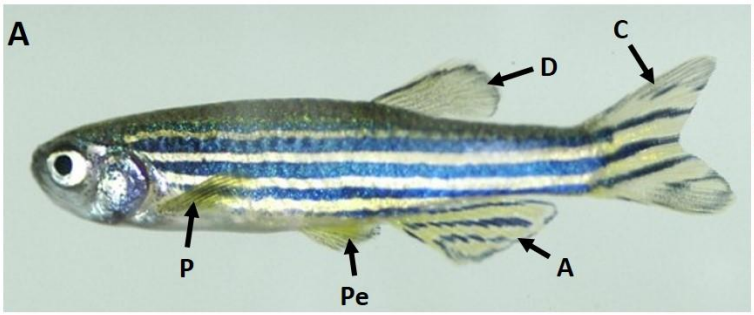
A
C
D
P
Pe
A

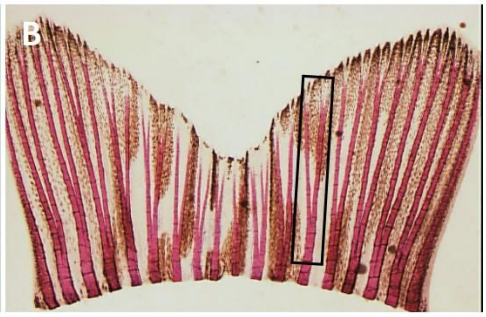
B

C

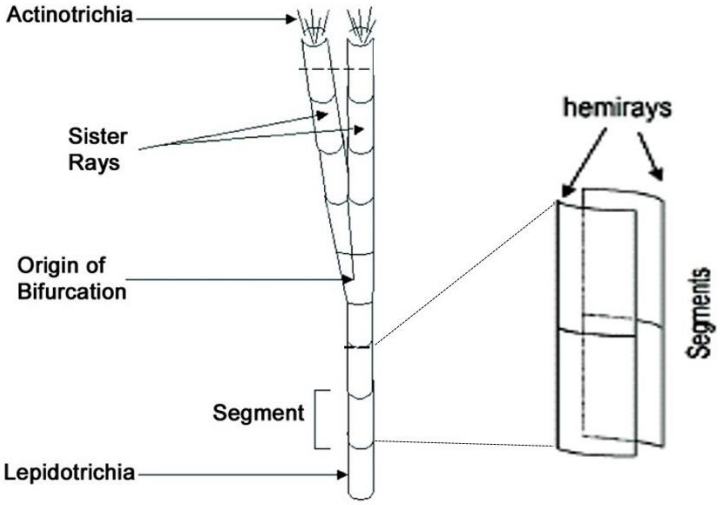
Actinotrichia
Sister Rays
Origin of Bifurcation
Segment
Lepidotrichia
hemirays
Segments

Figure 1.1 Representation of the zebrafish fins with specific focus on the lepidotrichia of the caudal fin. (**A**) Bright-field side view image of an adult zebrafish with all five fins labeled, pectoral fins (P), pelvic fins (Pe), anal fin (A), dorsal fin (D) and caudal fin (C). (**B**) A caudal fin stained with alizarin red showing ossified bone of the fin rays (lepidotrichia) (black box) seen in red. (**C**) Schematic for a single lepidotrichium (black box in B) obtained with permission from Quint and colleagues (Quint et al., 2002). Each lepidotrichium consists of multiple bone segments to make up one fin ray. Each ray is made up of two concave hemirays facing each other (zoom illustration in C). During development and regeneration, lepidotrichia undergo one or multiple bifurcations forming two sister rays.

1.2.2 Steps of regeneration of the caudal fin

The process of epimorphic regeneration in the caudal fin is responsible for the re-development of lost tissue due to direct amputation or injury. The regeneration begins with the healing of the wound right after amputation and then the fin begins regrowth to its normal length (Figure 1.2). The regeneration response is temperature dependent, and at 28.5 °C, full regeneration of lost tissue is seen after approximately three weeks. Such systematic and rapid regeneration is only seen after amputation of the exoskeleton. Fins that are amputated at the level of the endoskeleton generally do not regenerate. However, one study reported regeneration of the endoskeleton in 50% of cases and this regeneration was taking much longer time (approximately 51 days at 24 to 29 °C) (Shao et al., 2009). There are three fundamental hallmarks of regeneration. The process starts with wound healing followed by blastema formation and finally concludes with regenerative outgrowth (Poss et al., 2003).

A. Wound healing

Figure 1.3, shows a simple illustration of the three steps of regeneration after an amputation. The wound healing process is the first response to amputation or injury in the caudal fin. The closure of open blood vessels is almost immediate and that is why bleeding is limited (Figure 1.3, wound healing). There is a rapid migration and rearrangement of epithelial cells of the stump to the wound site to cover the wound. Within the time frame of 1 to 3 hours post amputation (hpa), a thin layer of wound epidermis begins to form. This wound epidermis then undergoes a maturation phase during the next 12 hpa (at 33°C), where it thickens and becomes multilayered by continuous cell migration (Poss et al., 2003). BrdU staining analysis has shown that this stage does not involve any cell proliferation (Poleo et al., 2001). At the same time as this thickening of the wound

epidermis is occurring, the mesenchymal tissue underneath is being disorganized and loosened, which allows for cell movements (12-24hpa). This disorganization and cell migration is thought to be the result of a response to signaling molecules released by the mature wound epidermis (Tal et al., 2010). The formation of the wound epidermis has been found to be essential for the regeneration process because it is necessary for the formation of the blastema (Schebesta et al., 2006).

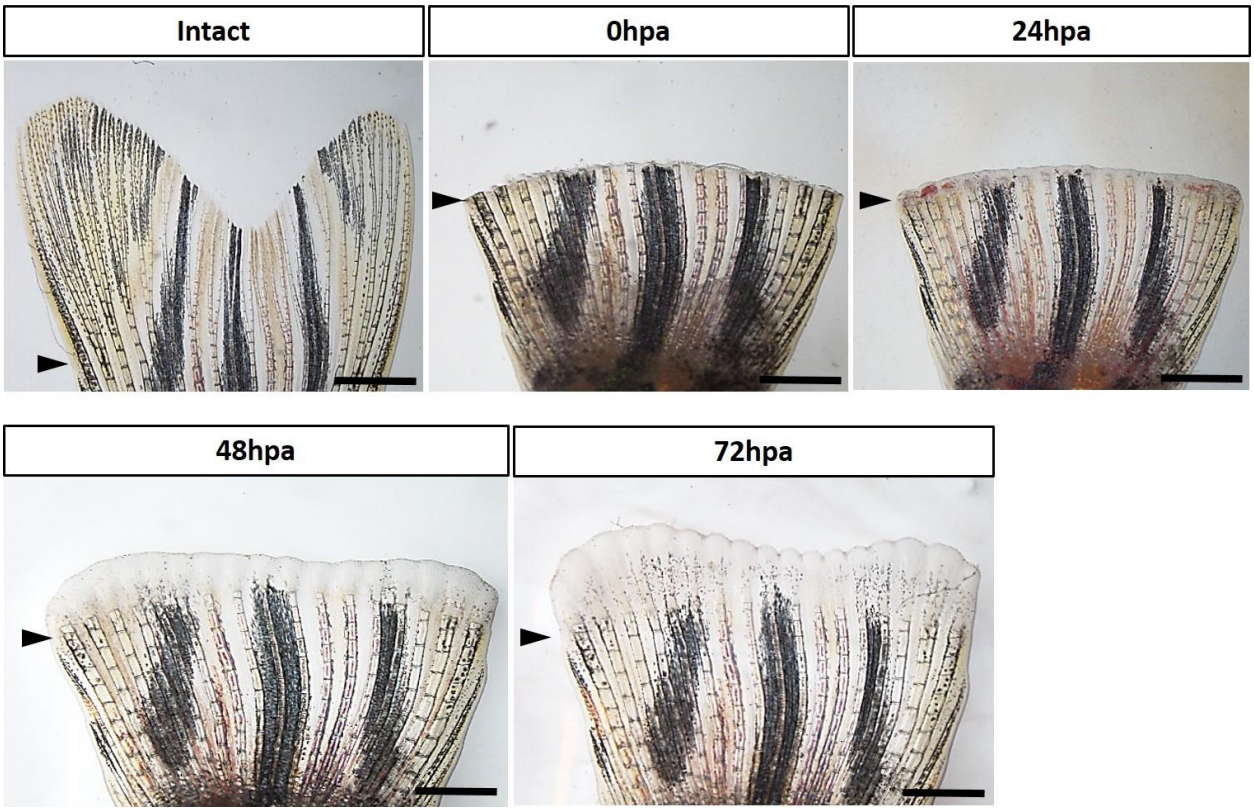
Intact
0hpa
24hpa
48hpa
72hpa

Figure 1.2. Time course of caudal fin regeneration during the first three days following amputation at 28.5°C. First panel: intact fin; following panels: 0hpa, 24hpa, 48hpa and 72hpa respectively. Black arrowhead indicates the level of amputation. Scale bar = 0.1 cm in intact fin image (0hpa) and 0.08 cm in all consecutive images.

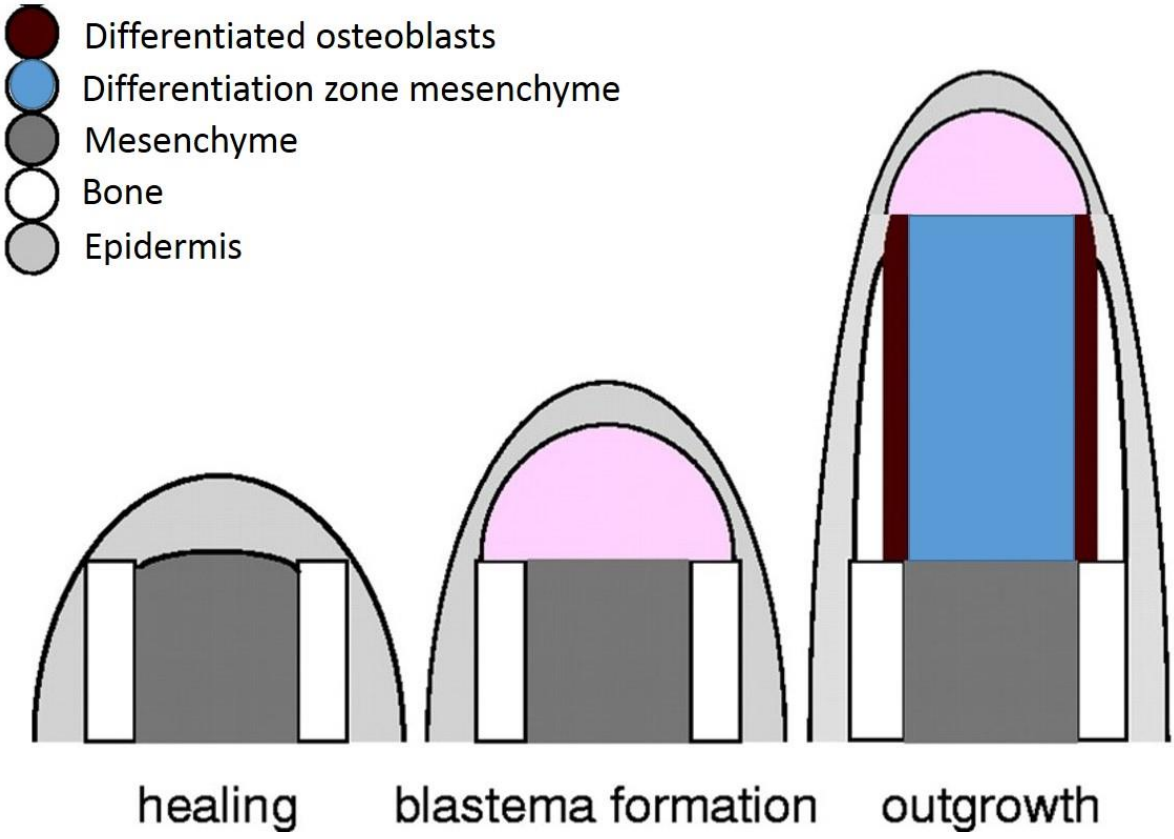
Differentiated osteoblasts
Differentiation zone mesenchyme
Mesenchyme
Bone
Epidermis
healing
blastema formation
outgrowth

Figure 1.3. A simple schematic representing the three steps of regeneration starting with wound healing then blastema formation and finally regenerative outgrowth. Initially the process begins with wound closure and the formation of the wound epidermis (Grey). The formation of the blastema is essential for the regeneration process (seen in pink). The regrowth of the lost tissue then follows by a process of differentiation and patterning (newly differentiated osteoblasts, which are the bone-forming cells are seen in brown and differentiation mesenchyme in blue). The figure is adapted with permission from Poss and colleagues (Poss et al., 2002).

B. Blastema formation and maturation

The next step is the formation of the blastema, which is a collection of heterogeneous mesenchymal-like cells located between the stump tissue and the wound epidermis (Figure 1.3). The mesenchymal tissue underneath the mature wound epidermis will undergo disorganization characterized by the migration of several cells to accumulate under the wound. These cells most likely undergo de-differentiation to form a pool of cells that is un-differentiated and is known as the blastema (Knopf et al., 2011, Stewart and Stankunas, 2012). The blastema forms the cell pool feeding the regeneration process (Singh et al., 2012). The cells of the blastema will proliferate continuously and will differentiate following different fates in regenerating lost structures. The cells of the blastema most likely come from different areas such as osteoblasts lining the surface of bone, cells of the connective tissue between the two rays, pigment cells, Schwann cells of the sensory nerves, endothelial cells forming the blood vessels and blood cells. The possibility of the involvement of progenitor stem-like cells is valid, but there is no evidence supporting the possibility that such cells are contributing to the formation of the blastema. However, it has been shown that regenerated melanocytes in the fin can arise from melanocyte stem cells (MSCs), rather than existing differentiated melanocytes (Rawls and Johnson, 2001, Tryon and Johnson, 2012). The formation of the blastema at around 24 hpa is a major requirement for regeneration (Poss et al., 2000). Upon maturation, the blastema can be divided into two compartments: the proximal blastema, which is made up of a dense and highly proliferative pool of cells and the distal blastema, which is composed of slowly cycling cells (Nechiporuk and Keating, 2002).

C. Regenerative outgrowth

In addition to the proximal and distal blastema, there is a third defined region that will appear in the regenerate called the “differentiation zone”. When un-differentiated cells leave the proximal

blastema, they will enter the differentiation zone and give rise to different cell types via re-differentiation, leading to the reestablishment of the lost organ (Figure 1.3). Throughout the regeneration process, the differentiation zone is located below the proximal blastema. It is unclear whether the blastema cells are multipotent meaning that they are able to give rise to cell types of multiple lineages that make up the fin. Several recent studies have shown that certain cells, such as the osteoblasts, are lineage restricted during regeneration (Jopling et al., 2010, Singh et al., 2012, Stewart and Stankunas, 2012). Defined lineage restriction occurs by a process of dedifferentiation followed by redifferentiation into the same original cell type. One example of these newly differentiated cells that appear within the differentiation zone are the osteoblast cells, which are an essential ingredient for the formation of new bones in the regenerate.

1.3 Bone development and ossification

The understanding of the process of bone formation in development and in regeneration is very important for the scope of my project. There are two known forms of bone ossification, endochondral ossification and intramembranous ossification.

The initial formation of bones begins with mesenchymal cells undergoing condensations. These condensations will either form a cartilage mold for the formation of bones as in the case of endochondral ossification or will undergo direct mineralization as in the case of intramembranous ossification. Initially during embryonic development, mesenchymal condensations begin to form the cartilage mold, which is then followed by the formation of the primary ossification center leading to the beginning of bone deposition (Kobayashi et al., 2002, Kronenberg 2006). During postnatal development, the bone must continue to grow, which leads to the formation of the

secondary ossification center allowing the longitudinal growth of the long bones (Chen et al, 2008).

1.3.1 Endochondral ossification

Much of the mammalian skeleton including long bones in the limbs are endochondral bones and derive from a cartilage intermediate template. During limb development, mesenchymal cells originating from the lateral plate mesoderm will condense and form a cartilage anlage composed of chondrocytes, that are cartilage-forming cells (Karp et al., 2000, Long et al., 2004, Mackie et al., 2008). These chondrocytes are surrounded by several layers of fibroblast-like cells making up the structure known as the perichondrium. Chondrocytes within the anlage are initially at the resting state and then begin the stage of continuous proliferation, which creates a stacked columnar organization as chondrocytes continue to proliferate (Kobayashi et al., 2002, Lu et al., 2013). The chondrocytes within the anlage are organized in a zonal growth plate fashion where the resting chondrocytes are at the distal growth plate towards the ends of the growing mammalian long bone and they have a round shape. Figure 1.4A shows a schematic of the formation the endochondral long bone and is a reference for the general distribution of cells in endochondral bone. The proliferating chondrocytes are aligned as columnar cells proximal to the resting chondrocytes and extending to the hypertrophic zone near the middle of the bone (Long et al., 2004). As chondrocytes move away from the zone of proliferation and exit the cell cycle, the chondrocytes begin to differentiate and become hypertrophic chondrocytes. Following hypertrophy, these chondrocytes that secrete the cartilaginous matrix will undergo apoptosis and will be replaced by osteoblasts (Long et al., 2004, Mackie et al., 2011). The osteoblasts are the bone-forming cells and their presence is concomitant to the invasion of vasculature from the surrounding tissue. The differentiating osteoblasts are responsible for the formation of the bone collar and the deposition

of bone (Kobayashi et al., 2002, Lu et al., 2013). The bone collar is like a cuff of deposited bone that forms around the cartilage model for support during development. Thus, in endochondral ossification, osteoblasts differentiation and bone deposition is closely coupled with chondrocyte maturation (Karp et al., 2000, Mackie et al., 2011).

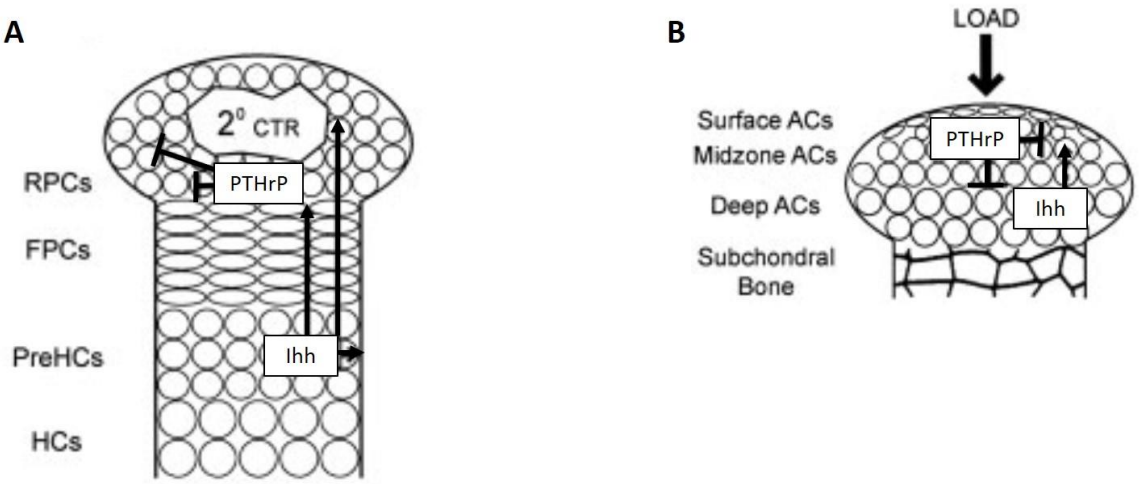

Growth plate **Articular cartilage**

Figure 1.4. The parathyroid hormone related protein (PTHrP) and Indian hedgehog (IHH) axis in the growth plate and articular cartilage. **A**: Round proliferative chondrocytes (RPCs), flat proliferative chondrocytes (FPCs), prehypertrophic chondrocytes (PreHCs), and hypertrophic chondrocytes (HCs) are indicated in the growth plate of endochondral bone during post-natal development. **B**: The distribution of articular chondrocytes (AC) in the different zones of the long bone epiphysis. The arrow with "load" represents the mechanical stimulation on the articular cartilage. Lines with perpendicular dash indicate inhibitory effects by PTHrP or IHH and arrows indicate stimulation effects. Adapted with permission from Chen et al., 2008.

1.3.2 Intramembranous ossification

In intramembranous ossification, there is no need for a cartilage intermediate. Intramembranous bones, such as craniofacial bones, arise in a direct process from the differentiation of mesenchyme, which was initially compacted into sheets or membranes (Abzhanov et al., 2007, Franz-Odendaal, 2011). The compacted mesenchymal cells differentiate into osteoblasts, forming the primary ossification center. The osteoblasts begin to release osteoid to form the hard center, which continues to grow as more osteoid is released (Franz-Odendaal, 2006). The osteoid will then get mineralized, thereby accumulating hard bone around embryonic blood vessels (Lenton et al., 2011). The vascularized mesenchyme external to the woven bone will then condense and become the periosteum (Franz-Odendaal, 2011). These details are mostly describing intramembranous bone of mice because this model is where most of the studies have been done.

1.4 IHH and PTHrP Signaling in Development

Indian hedgehog (IHH) and parathyroid hormone related protein (PTHrP), two secreted molecules, acting as paracrine factors that have been implicated in bone development both during embryonic and post-natal stages of life. In addition, they are also implicated in bone remodeling, especially at the level of joints and tendon insertion sites, based on mechanical stimuli. These roles will be covered in the upcoming sections. Thus, as mentioned earlier, in endochondral ossification, there is a cartilage intermediate which is formed by chondrocytes. The roles of *Pthrp* and *Ihh* genes are achieved by feedback loop interactions between the two factors, which ensures that there is a

tight control between the level of chondrocyte proliferation and differentiation in growing bones (Kronenberg, 2006, Mackie et al., 2008). However, the point of interest here is that these genes, which are well understood as chondrogenic markers in endochondral bone, are also expressed in intramembranous bone (Avaron et al., 2006, Abzhanov et al., 2007). This is why I went on to investigate the roles of PTHrP and IHH in the lepidotrichia of zebrafish, which develop through intramembranous ossification. The next few sections will introduce PTHrP and IHH and discuss their roles in development.

1.4.1 Overview of Hedgehog Signaling Pathway

The Hedgehog signaling (Hh) pathway was first identified in *Drosophila melanogaster* and is largely studied in this species (Nusslein-Volhard and Wieschaus, 1980). HH is a secreted protein and it interacts with a 12-pass transmembrane protein called Patched (PTC). In *Drosophila melanogaster*, in the absence of Hh ligand, Hh receptor Ptc is inhibiting a 7-pass transmembrane protein called Smoothened (Smo). When Smo is inhibited, it is located in the cytoplasm of cells and the zinc finger transcription factor *Cubitus interruptus* (Ci) is forming a complex with Costal2-Fused (Cos2-Fu). This leads to the phosphorylation and processing of Ci (Ingham and McMahon, 2001). The Ci N-terminal fragment accumulates and enters the nucleus to act as a transcriptional repressor. In this case, the target genes of the Hedgehog pathway are not transcribed. When Hh is present, the binding of Hedgehog to its receptor Ptc leads to the internalization of Ptc. Smo is no longer inhibited by Ptc and its cytoplasmic tail will be phosphorylated by PKA and CKI. This phosphorylation leads to the activation and accumulation of Smo on the cell surface. This accumulation leads the membranous Smo to interact with Cos2-Fu-Ci cytoplasmic complexes to recruit Cos2-Fu complexes away from the zinc finger transcription factor Ci (Ho and Alman 2010). The full length Ci is no longer phosphorylated and processed to its N-terminal inhibiting form, and

is now able to translocate to the nucleus under its full length version, thus acting as a transcriptional activator. The pathway is rendered active and *hedgehog* target genes are transcribed.

In mammals, there are three Hedgehog orthologs: Sonic Hedgehog, Indian Hedgehog and Desert Hedgehog, respectively SHH, IHH and DHH (Echelard et al., 1993). The regulation of SMO localization by PTC1 is mostly conserved between vertebrate and non-vertebrate species. The vertebrate Hedgehog proteins control gene expression through the processing of the vertebrate homologs of Ci: the GLI transcription factors (Ingham and McMahon, 2001). GLI2 and GLI3 both act in a similar way to Ci, being either stabilized under their full-length form to act as transcription activators, or being cleaved to act as transcriptional repressors (Sasaki et al., 1999). GLI1, however, is lacking the proteolytic cleavage site and can only act as a transcriptional activator (Hynes et al., 1997; Aza-Blanc et al., 2000). The Hh proteins share a high degree of homology which predicts at least a partial redundancy of function. However the *Hedgehog* genes show different patterns of expression and play different roles during development (Ho and Alman, 2010).

This short introduction shows how the *Hedgehog* gene family signaling pathway works. With regards to our gene of interest, *Ihh* is expressed by prehypertrophic and hypertrophic chondrocytes in endochondral bone (Mackie et al., 2008). As will see later on, *Ihh* is also expressed in bones that develop through intramembranous ossification (Avaron et al., 2006, Abzhanov et al., 2007). In zebrafish, there are two *ihh* genes (*ihha* and *ihhb*) and two receptors (*ptch1* and *ptch2*), which will be discussed later in more detail.

1.4.2 Overview of *Pthrp*

My second gene of interest involved in the development and growth of endochondral bone is *PTHrP*. This gene is expressed by proliferating chondrocytes.

The parathyroid hormone related protein (PTHrP) was discovered in 1987 in humans as the circulating peptide responsible for the syndrome of humoral hypercalcemia of malignancy (HHM; Moseley *et al.,* 1987). PTHrP and parathyroid hormone (PTH), the main hypercalcemic hormone in vertebrates, evolved from a common, ancestral gene. Within a species, the two proteins share a high, approximately 70% homology in the N-terminal amino acid (aa), and they bind to a common *PTH/PTHrP* receptor (Juppner *et al.,* 1991). PTHrP is strongly conserved among mammalian species, which indicates its importance in mammalian physiology (Abbink and Flik, 2007). For example, human, chicken and rodents have 98% identity within the first 111 residues of PTHrP, while the average protein is 85% identical between chickens and humans (Lagerstrom et al., 2006). PTH is secreted by the parathyroid gland, but *PTHrP* is expressed in a variety of tissues, including many epithelia (De Papp and Stewart, 1993). PTHrP is an autocrine/endocrine regulatory factor with a number of functions during development (Kronenberg, 2006). These functions include the formation of mammary glands (Wysolmerski et al., 1998), driving the eruption of teeth (Suda et al., 2003) and, most importantly, regulating the chondrocyte differentiation program in endochondral bone (Vortkamp et al., 1996). Unregulated paracrine secretion of PTHrP is responsible for a type of tumor that causes elevated blood calcium levels, which is a condition called humoral hypercalcemia of malignancy (HHM) (Yan et al., 2012). In zebrafish, there are two *pthrp* genes (*pthrp1* and *pthrp2*) and three *pthrp receptor* genes (*pth1r, pth2r* and *pth3r*).

1.5 PTHrP and IHH in Bone

Here I will discuss details of the parathyroid hormone related protein (PTHrP) and indian hedgehog (IHH) feedback loop in the development of mammalian endochondral bones. There are other factors that play important roles in bone development like the bone morphogenic proteins (BMPs), fibroblast growth factors (FGFs), sonic hedgehog (SHH) and the Wnt signaling pathway (Minina et al., 2002). However, my focus here will be directed towards PTHrP and IHH and their roles in development, with specific focus on bones.

1.5.1 PTHrP and IHH at the growth plate

During embryogenesis initial bone formation starts with the primary ossification center as described above and during post-natal life, bones continue to grow after the formation of the secondary ossification center and the growth plate. This section will focus on the interactions at the growth plate. Those interactions represent a major premise for my first hypothesis. At the growth plate in endochondral bone, there are at least three morphologically distinct groups of chondrocytes. These three groups of chondrocytes are the round proliferating chondrocytes, flat columnar chondrocytes and the hypertrophic chondrocytes. The round proliferating chondrocytes and the flat columnar chondrocytes make up the reserve zone, which provides the bone with a continuous pool of proliferating chondrocytes for growth (Figure 1.4A). The round chondrocytes proliferate and differentiate to flat columnar chondrocytes, which proliferate further to form orderly columns (Kronenberg, 2006). These cells will eventually stop proliferating and differentiate into non proliferating hypertrophic chondrocytes. The three types of chondrocytes are separated by well-defined borders throughout the endochondral ossification process due to a tight

regulatory program (Kobayashi et al., 2002). PTHrP and IHH are two major players in this tight positional regulation. PTHrP is released by the round flat chondrocytes and acts on all adjacent chondrocytes expressing the PTHrP and PTH receptors, which are expressed in the regions of proliferating columnar chondrocytes and the prehypertrophic zone (Mackie et al., 2008). PTHrP enhances proliferation by preventing cells from exiting the cell cycle, which inhibits hypertrophy and differentiation. This allows for the maintenance of the proliferative pool of chondrocytes and limits the transition towards hypertrophy, which is when cells begin to express *Ihh*. As chondrocytes move farther, they begin to escape the control of PTHrP and start exiting the cell cycle to undergo early stages of hypertrophy and initiate *Ihh* expression (Mackie et al., 2008). Prehypertrophic and hypertrophic chondrocytes release IHH, which acts on IHH receptor (Patched 1, PTC1) expressed by round proliferating chondrocytes and flat proliferating chondrocytes and enhance their proliferation. In addition, IHH stimulates these cells to continue releasing PTHRP. Therefore, IHH is involved in the positive regulation of the number of differentiating chondrocytes by enhancing proliferation and by inducing the continued release of PTHRP, but the exact mechanism of this regulation is poorly understood (Lenton *et al.*, 2011). Therefore, the release of IHH forms a feedback loop with PTHRP, which regulates the onset of hypertrophic differentiation, by creating a fine line between the zone of proliferation and the zone of differentiation (Vortkamp et al., 1996). Eventually, hypertrophic chondrocytes will further differentiate and become mature. Mature chondrocytes will then mineralize the surrounding matrix and undergo apoptosis. In parallel, osteoblasts, which are the bone-forming cells, will also differentiate at the periphery of the cartilage neighboring the mineralized hypertrophic chondrocytes. The mineralized cartilaginous matrix will later be invaded by vascular tissue. Osteoblasts coming in with vascular tissue and the perichondrium will deposit bone matrix onto the degraded mineralized cartilaginous

matrix to form the bone (Gerber and Ferrara, 2000, Mackie *et al.*, 2008). In addition to promoting proliferation, IHH is also required for osteoblast development and growth along the bone axis in endochondral ossification (St-Jacques *et al.*, 1999).

Both *PTHrP* null and *PTH*/*PTHrP* receptor null mice develop chondrodysplasia because of decreased numbers of mitotically active chondrocytes, causing premature hypertrophic differentiation and premature ossification (Karaplis et al., 1994, Lanske et al., 1996). The *Ihh* null mouse phenotype is perinatal lethal (Long et al., 2004). The mice show reduced chondrocyte proliferation and absence of differentiated osteoblasts, leading to foreshortened bones as the most obvious phenotypic manifestation (Karp et al., 2000). On the other hand, over expression of *Ihh* forms shorter and thicker bones due to an inhibition of chondrocyte differentiation. In contrast, overexpression of *Pthrp* leads to an increased pool of proliferating chondrocytes that cannot exit the cell cycle.

1.5.2 PTHrP and IHH in articular cartilage

The second interaction between IHH-PTHrP axis is the articular cartilage, which is the second population of *PTHRP* expressing cells that form after the formation of the secondary ossification center. In the articular cartilage, *Pthrp* is expressed by surface articular chondrocytes and *Ihh* is expressed by the deep articular chondrocytes (Mackie et al., 2011) (Figure 1.4B). This figure illustrates the location of chondrocytes at the area of articular cartilage at the ends of long bones. There appears to be a different regulatory mechanism here in the form of external loading. The primary stimulator and regulator for PTHRP is mechanotransduction (Chen et al, 2008). In the articular cartilage, PTHRP expression is maintained high in the surface and midzone articular chondrocytes if the joints are loaded, while *Ihh* expression in prehypertrophic chondrocytes in the

deep zone would be presumably minimal. This seems to be the only example where the main stimulus of the PTHrP/IHH axis is mechanical. One of the hypotheses about the presence of PTHRP in articular cartilage is because this gene is involved in joint specification (Mackie et al., 2011). Other data suggests that PTHrP is not involved in joint specification, but rather, mainly involved in regulating the maintenance of articular chondrocytes (Chen et al., 2008).

1.5.3 Recent work on tendon and ligament insertion sites

Other recent studies have shown that *PTHrP* is expressed in the tendon and ligament insertion sites (entheses) of bones. In a study by Wang and colleagues, *PTHrP* was found to be expressed in the fibrous layer of the periosteum and the periosteal component of fibrous insertion sites (Wang et al., 2013). It was shown to be involved in the regulation of modeling of cortical bone surfaces at fibrous insertion sites during growth. The induction of this regulation by PTHrP seems to be mechanically activated to regulate a balance between osteoblasts and osteoclasts (bone resorption cells). PTHrP mediates this role by osteoblast/osteoclast recruitment to ensure proper balance between bone building and resorption based on the load on the insertion site (Chen et al., 2007).

1.5.4 Ihh and Pthrp signaling in zebrafish

In zebrafish, due to the genome duplication that occurred after the divergence of the teleost lineage from the tetrapod lineage, the presence of gene duplicates is a common feature (Gensure at al. 2004). There are two indian hedgehog genes (*indian hedgehog a, ihha* and *indian hedgehog b, ihhb)* and two parathyroid hormone related protein genes (*parathyroid hormone related protein 1, pthrp1* and *parathyroid hormone related protein 2, pthrp2*) (Avaron *et al.,* 2006 and Yan *et al.,* 2012). Similar to the expression of *Ihh* in tetrapods, zebrafish *ihha* has been observed in a few cells of the parachordal cartilage in embryos at 4 days post fertilization (dpf). These cells also

expressed *col10a1* gene coding for cartilaginous matrix and are relatively large, suggesting that they correspond to pre-hypertrophic or early hypertrophic chondrocytes (Avaron et al., 2006). Also, consistent with their role during endochondral ossification in tetrapods, *ihha* and *ihhb* are expressed in several cartilaginous elements in 6dpf embryos. However, *ihha* is also expressed during dermal bone formation of the scales and during fin ray regeneration in early differentiating osteoblasts (Avaron et al., 2006). These were identified as osteoblasts because they express osteoblast markers such as *runx2a* and *runx2b* (Smith et al., 2006).

Unlike mammals, the role of Pthrp in zebrafish has not been studied in great detail and there is limited information in regards to its expression profile and function. The limited information that is available has been published in recent years. Out of the two, Pthrp1 shows more similarity to the human PTHrP than Pthrp2 (Yan et al., 2012). One prevailing hypothesis regarding the function of Pthrp in zebrafish is that it is an endocrine hormone involved in regulating serum calcium homeostasis and osmoregulation. This hypothesis is supported by the fact that teleost serum shows high plasma Pthrp levels (Abbink and Flik, 2007). A recent study shed light on an additional proposed function for Pthrp in zebrafish by describing it as a paracrine hormone necessary for chondrogenesis and osteogenesis similar to mammals (Yan *et al.,* 2012). Zebrafish *pthrp* co-orthologs are expressed in the pancreas, spinal cord, bone, cartilage and developing teeth, which is similar to the expression of the mammal orthologs. Specifically, with regards to bone formation, Yan and colleagues showed that there is an upregulation in the transcripts of *runx2b* in *pthrp1* knockdown embryos. This is consistent with previous observation regarding mammalian PTHrP and its role in slowing chondrocyte maturation via inhibition of Runx2 (Iwamoto et al., 2003). In zebrafish, Runx2a and Runx2b are transcription factors that are expressed in osteoblasts

in the early maturation stage and they are essential for the osteoblast maturation program (Singh et al., 2012).

1.6 Background information regarding the project

Thus far, we know that the lepidotrichia of the zebrafish exoskeleton develop through intramembranous ossification, which means that there is a direct mineralization of bone matrix secreted by the specialized osteoblasts without the presence of a cartilage intermediate. Hence, the absence of cartilage means an absence of chondrogenic markers in dermal bone of fin rays. However, our work and the work of others found chondrogenic markers expressed in areas where there is no cartilage and where bone development is entirely of intramembranous origin. For example, Abzhanov and colleagues have shown that *Ihh* and *Pthrp*-receptor are expressed in the craniofacial bones of chick and mouse embryos (Abzhanov *et al.,* 2007). The expression of these markers was seen through *in situ* hybridization analysis of the dentary bone in these embryos. In addition, Lenton and colleagues performed more in depth work with regards to the expression of *Ihh* and its regulatory role in intramembranous ossification in a mouse model (Lenton et al., 2011). They showed that IHH is an important positive regulator of cranial bone ossification (Lenton *et al.,* 2011). They showed that *Ihh* null mice embryos have defects in the intramembranous ossification and secondary suture. More importantly, with regards to zebrafish, previous work in our lab has shown that there are chondrogenic markers expressed in the intramembranous bony rays of fins. During caudal fin regeneration, *ihha* is expressed in regenerating fin rays in newly differentiating osteoblasts (Avaron et al., 2006). In adult zebrafish, although these markers are

expressed, their roles and interactions in skeletogenesis is still poorly understood especially in the process of regeneration.

Knowing this information, our lab was interested in probing into the role of Ihha and Pthrp1 during regeneration of caudal fin rays. The very first work performed on this subject was to analyze the expression of *pthrp1* in regenerating caudal fin rays especially after knowing that previous work in our lab showed a defined expression profile for *ihha*. The first analysis of the expression pattern of *pthrp1* was done by Leona Probst, a previous student in our lab, using *in situ* hybridization (L. Probst, unpublished data). The expression profile witnessed was a horizontal line across the distal end of the blastema in whole-mount caudal fin regenerates. The probe used for *in situ* hybridization was obtained by amplifying a cDNA segment obtained by reverse transcriptase PCR on RNA preparation from 4dpa fin regenerates and using primers designed for *pthrp1* (also known as *pthrpa*) (*pthrp1*- NM_001024627.2). Using *in situ* hybridization on whole-mount and sections, Leona found that the expression pattern of *pthrp*1 overlaps with the expression domain of *evx1* (Figure 3.1B-E). The latter encodes for a homeodomain containing transcription factor that is expressed in multiple tissues during vertebrate development. In zebrafish, it is expressed in the central nervous system, proctodeum and the fins (Borday et al., 2001, Schulte et al., 2011). Later on, a study by Schulte and colleagues showed that zebrafish *evx1* homozygous mutant lack any joints in their fins suggesting that *evx1* is required for the formation of joints in the zebrafish exoskeleton of fins (Schulte et al., 2011). This finding was very interesting for us because our previous results have shown the co-localization of *evx1* and *pthrp1*, which could indicate a potential interactive role between the two.

With all this information in hand, I set out to investigate the role of these two genes (*pthrp1* and *ihha*) with regards to their involvement in zebrafish fin ray regeneration by performing

expression and functional analysis. Knowing that there was a duplication of the genome compared to the tetrapod lineage plus my review of the literature, analysis of the Ensembl Genome Browser database showed that there are two genes in the zebrafish *pthrp* family (*pthrp1* and *pthrp2*) and there are three receptor (*pth1r*, *pth2r* and *pth3r*) genes. In addition, there are two *ihh* genes (*ihha* and *ihhb*) and there are two receptors (*ptch1* and *ptch2*). I started my analysis with the closest orthologs to the mammalian genes, which were *pthrp1* and *ihha*, and also analyze the *pthrp* receptors.

1.7 Hypothesis and objectives

As stated before, the expression of *ihha* was observed in newly differentiated osteoblasts in the differentiation zone of regenerating fins. Also, preliminary work on the *pthrp1* gene showed an expression profile that was visible on the regenerate portion of caudal fin at the distal end of the blastema as a distinct horizontal line of cells. This picture seems to resemble the well described scheme for endochondral ossification at the growth plate. The horizontal line of *pthrp1* expressing cells that are located at the distal tip of regenerate seem to morphologically resemble the location of the PTHrP releasing round proliferating chondrocytes of the growth plate and the newly differentiated osteoblasts expressing *ihha* may resemble the osteoblasts of the perichondrium or the hypertrophic chondrocytes. One hypothesis was that Pthrp1 and Ihha may play an essential role in the regeneration of bones in the caudal fin of zebrafish possibly in a similar fashion to the role they play in endochondral ossification. Therefore, the interactions of Pthrp1 and Ihha in regenerating fin rays would resemble those occurring at the growth plate of mammalian endochondral bones. Hence, if the function of these genes is perturbed then bones will not

regenerate properly since the balance between proliferation and differentiation cannot be established for proper bone growth. Another hypothesis was that Pthrp1 may be involved in the formation and maintenance of joints in newly regenerating fin rays. My reasoning for this was the expression profile of *pthrp1* is in a horizontal line at the level of newly forming joints and it is co-localizing with *evx1*, which is required for the formation of joints in caudal fin rays.

Specific objectives:

- The first objective was to analyze the expression pattern of *pthrp1* and *ihha* using *in situ* hybridization and reverse transcriptase PCR
- The second objective was to perform a functional analysis using morpholino knockdown experiments targeting *pthrp1* and *ihha*
    - Analysis of morpholino injected fins and embryos for defects in the morphology specifically with regards to the formation of bones such as bone deformities, regenerated bone length and area of regenerative outgrowth.
- The third objective was to analyze the expression of the other member of the *pthrp* gene family, *pthrp2*, and the receptors (*pth1r, pth2r* and *pth3r*) using RT-PCR and *in situ* hybridization.

2. Materials and Methods

2.1 Animal Care

The zebrafish were kept in an aquatic facility with continuous running water at a temperature of 28.5 °C with a photoperiod that consists of 14 hours of light and 10 hours of darkness with regular cleaning and feeding (Westerfield, 1995). Embryos were raised in incubators at 37 °C for the first 5-7 days of their lives in petri dishes with nutrient medium then they were moved to an aquatic facility. In the aquatic facility, the embryos were kept in small tanks with the same nutrient media, which was changed on a daily basis. When the embryos were large enough, they were transferred to juvenile tanks in the main system. In the amputation operations, I usually performed the experiments outside the aquatic facility and then returned the fish to their tanks in the facility.

2.2 Fin amputation

The amputations were performed on the caudal fin of fish that were 12 weeks of age or older. Fish were collected from a tank using a small fish net and placed in a bowl with water containing 0.17 mg/ml Tricaine (ethyl-aminobenzoate; Westerfield, 1995) to immobilize the fish and reduce any possible pain or discomfort caused by the procedure. Using a scalpel blade, the caudal fins were amputated in a straight line one or two segments proximal to the first branching point of the lepidotrichia. The fish were then returned to their tanks where they rapidly recovered with little bleeding and no signs of obvious pain. The fin regenerates were then collected at desired

time points by cutting the regenerate in a straight line one segment proximal to the initial amputation line.

2.3 RNA Extraction

Fin regenerate was collected and placed directly into an eppendorf tube and then the tube was placed into liquid nitrogen to preserve the RNA. 1ml of TRIzol reagent (Catalogue # 15596-026, Invitrogen) was added to about 10 regenerates at 4dpa. The tissue sample was homogenized by pipetting in and out using large tips followed by smaller tips. The homogenized samples were incubated for 5 minutes at room temperature to allow complete dissociation of nucleoprotein complex. The RNA was then extracted using 200 µl of chlorofom for each 1 ml of Trizol and the solution was vortexed for 15 seconds. The tubes were incubated at room temperature for 2-3 minutes and then centrifuged for 10 minutes at room temperature at 12500 rotations per minute (RPM). The aqueous phase was then precipitated by addition of 500 µl of isopropanol and tubes were incubated at room temperature for 10 minutes and then spun for 15-20 minutes at 12500 RPM at a temperature of 4°C. Finally, the precipitate was washed twice with 500 µl of 70% ethanol in diethylpyrocarbonate (DEPC) water. The pellet was resuspended in 20 µl of DEPC water and incubated for 10 minutes at 60 °C. The RNA was stored at -80°C.

2.4 cDNA synthesis

The synthesis of cDNA was performed using QuantiTect Reverse Transcription Kit (catalogue # 205310, QIAGEN). I followed the protocol supplied with the kit using RNA extracted in the previous step.

2.5 RT-PCR

RT-PCR experiments was performed using the Phusion PCR Master Mix (Thermo Scientific) and using and an S1000 Thermal Cycler (BIORAD). The PCR program was composed of a denaturation phase at 95 °C for 5 minutes, followed by an annealing phase at 55 °C for 30 seconds and finally an extension at 72 °C for 10 minutes. 35 cycles of amplification were used. Primers used are described in the probe design section.

2.6 Subcloning fragments into pDrive vector

The synthesized cDNA prepared from RNA of embryos and fin regenerates was used to amplify fragments located between the selected primers using PCR technology. Once the desired fragment was detected as amplified, the fragment was gel-purified and inserted into a suitable vector for future applications.

PCR products were initially purified using Sigma Spin Post-Reaction Clean up Columns (Sigma-Aldrich S5059-70E). Each purified PCR product was then ligated to pDrive cloning vector using the QIAGEN PCR cloning kit (catalogue # 231122, QIAGEN). I followed the protocol that was supplied with the pDrive cloning vector. The ligation was performed overnight at 16°C in a water bath.

The next day, the ligation mix was used to transform electrocompetent *E.coli* cells. X-10 electrocompetent cells (-80°C) were thawed at room temperature and then kept on ice. Next, I added 3µl of [1ng/ µl of the plasmid DNA] of the ligation mix to 40 µl of electrocompetent cells.

The mixture was incubated on ice for 10 minutes and then transferred to an electroporation cuvette. The cuvette was placed in an electroporator and the cells were pulsed. Following electroporation, 1ml of SOC media (SOB medium [(tryptone 20g, yeast extract 5g, NaCl 0.5g, 250mM KCl 10ml, 1M $MgCl_2$ 10ml and H_2O) plus 20mM glucose)] was added and the solution was incubated in a 5 ml tube for 1 hour at 37°C with moderate shaking. After incubation, the bacterial solution was transferred to a 1.5 ml tube and centrifuged at 8000 rpm for 30 seconds. Most of the liquid medium was discarded leaving only 200 µl, which was used to re-suspend the pellet before it was plated on an LB media agar plate with kanamycin or ampicillin antibiotics.

2.7 Morpholino injection

My method of morpholino injection was based on our lab protocol and some guidance from Thummel and colleagues in their paper for *in vivo* electroporation (Thummel *et al.,* 2006). The adult fish were initially anesthetized in Tricaine before the amputation of the distal portion of the caudal fin one to two segments proximal to the first lepidotrichia branching point. Once amputation was completed, the fish were returned to the water tank at 33°C. After 48 hours, the fish were re-anesthetized and injected with morpholino (MO) directly in the blastema of regenerating fins (experimental morpholino = dorsal, control morpholino = ventral). The injection was tested in both lobes of the fin and there was no difference detected between the two lobes, so injection was fine in both the dorsal or the ventral lobe. My initial method involved the injection of the *ihha* or *pthrp1* morpholinos into the dorsal side of the fin and then I immediately followed that by electroporation. Once the targeted morpholino injections were done, I re-anesthetized the fish and injected the ventral side with the standard control morpholino (CCTCTTACCTCAGTTACAATTTATA), and

followed that by an immediate second electroporation. The injection was performed using a NARISHIGE IM-300 microinjector, with a pressure of 102 psi and for 30 msec/injection. The morpholinos (Gene Tools, Inc.) used were a *pthrp1* translation-blocking MO (5'-CCCGTC-TGCAACACAACATCCTCAT), an *ihha* translation-blocking MO (5'-GGGAGACGCATTCCAC-CCCAAGCGG) and the Gene Tools standard control morpholino. Each morpholino came as a powder with a 3' fluorescein tag and it was suspended in water (1mM concentration). I aimed my injection to localize in the area of the regenerative tissue just distal to each bony ray so that it would correspond to the blastema of the regenerate. I injected into the long four to five outer rays of each fin excluding the outer most ray from my count. The injection volume was approximately 90 nl. Following the injection of morpholino, I immediately conducted the electroporation for the both the dorsal and the ventral sides of the fin to control for non-specific electroporation effects. For the electroporation I used a Tweezertrodes Kit, 3mm Platinum (BTX Harvard Apparatus) that were covered with any type of medical ultrasound gel on both sides of the clamp to localize the pulses to approximately one-half of the fin (dorsal and ventral). The electrodes were connected to ECM 830 Square Wave Electroporator (BTX Harvard Apparatus) and the parameters used were 15 consecutive 50-msec pulses, at 15 V with a 1-sec pause between pulses. After the electroporation was completed, the fish were returned back to the tank and observed at 72hpa to assess the efficiency of the injection and begin further analysis.

2.8 Microscope Imaging

The imaging was done using a dissection microscope (Leica MZ FLIII) with an installed digital camera (Sony 3CCD Color Video Camera). The photographs were captured on a standard

computer with AxioVision Imaging software. Bright-field imagery required an exposure of approximately 6msec. For fluorescence imaging, we used the integrated FLUOIII filter system to visualize the samples. Fluorescent pictures of whole-mount caudal fin require an average exposure time of 700ms.

2.9 Preparation of Antisense RNA probes

Antisense RNA probes for *in situ* hybridization were synthesized *in vitro* from a linearized DNA template. The synthesis reaction was composed of 1μg DNA template, 2 μg NTP labelling mix [10mM ATP, 10mM CTP, 10mM GTP, 6.5mM UTP and 3.5mM DIG-11-UTP (Roche)], 20 units of RNAsin (Fermentas) and 20 units of the appropriate RNA polymerase, Taq Polymerase (Roche). The mixture was brought to a volume of 20 μl using DEPC treated water. Next, the mixture was incubated in a water bath at 37 °C for two hours. The synthesized probe was then purified using a Sigma Spin Post-Reaction Clean up Column (Sigma-Aldrich S5059-70E) in accordance with the manufacturer guidelines. The purification step was followed by RNA concentration and quality analysis by mixing 1 μl of probe solution with 3 μl of 2xRNA loading dye and 5 μl of DEPC water. The mix was then heated at 70 °C for 5 minutes and then chilled on ice so that it could be run on a 0.8% RNAse free agarose gel. Finally, to ensure the preservation of the RNA probe, 9μl of RNA Later (Sigma) (RNA preservative) and 1μl of 0.5M EDTA were mixed with the original probe mix and placed in a freezer at -80 °C. The average RNA probe concentration obtained after finishing this protocol was approximately 200ng/μl.

The mRNA sequences used to design the RNA probes were accessed from Ensembl Genome browser with the accession numbers (*pthrp1*- NM_001024627.2, *pthrp2*- NM_001043324.1, *pth1r*- AF132084.1, *pth2r*- NM_131377.1, *pth3r*- NM_131378.1). The primer sequences used were:

pthrp1 (forward primer-5'CGTAATGCTGAGCCGGACA3', reverse primer-5'TCACTGAACGCTTCATTCGGCT3'), *pthrp2* (forward primer-5'AGCAGACAACGGCGTTCAGT3', reverse primer- 5'AGCGTGTGCCTTCCAAATGC3'), *pth1r* (forward primer- 5'TGTGCCAAATTCTTCCCCCA3', reverse primer-5'GAGCCGTCGAAAGTATCCGA3'), *pth2r* (forward primer-5'CTTCTGTTCTCCGCGTCAGT3', reverse primer- 5'ATGCATGTGCTGCATGGTTG3'), *pth3r* (forward primer- 5'AAGCATGGTGTCAGTGGAGG3', reverse primer-5'ACGCGTATCCTCTGTGGTTG3').

2.10 Whole-mount *in situ* hybridization

The *in situ* hybridization experiment on whole mount tissue was performed in accordance with the protocol provided by Laforest and colleagues (Laforest et al., 1998). After amputation fins were fixed in a solution of phosphate buffered saline (PBS) containing 4% paraformaldehyde (PFA) at 4 °C overnight. The next day, the fins were washed twice with PBS for 5 minutes, twice with 100 % methanol for 5 minutes and then stored at -20 °C. On the first day of *in situ*, all solutions and washes were prepared using DEPC water to keep an RNAse free environment. The entire procedure was performed using six well plates (NUNC Brand Products) with the fin tissues placed in plastic baskets with a mesh base. The samples were taken out of methanol and rehydrated in a

series of 5 minute washes with different dilutions of methanol and 1xPBS (75% MeOH:25% PBS, 50% MeOH:50% PBS, 25% MeOH:75% PBS). Next step was to wash the samples 3 times with PBST (1x PBS, 0.1% Tween-20) for 5 minutes each. The next step was to permeabilize the fins in 20μg/ml proteinase K (Invitrogen) for 30 min. The samples were then washed twice for 5 minutes each in PBST. The next step was a fixation step in 4% PFA for 20 minutes and followed by two 5 minute washes in PBST. Samples were then placed in acetylation mix, which consists of 37.5 μl of triethanolamine and 8.1 μl acetic anhydride in 3 ml of DEPC water for 10 minutes. Another wash in PBST followed for 10 minutes. The next steps were pre-hybridization and hybridization, which were performed in eppendorf tubes instead of the 6 well plates. The samples were pre-hybridized for 2-3 hours at 70 °C in a hybridization mix containing 50% deionized formamide, 5x SSC (20x SSC stock solution; 3.0M NaCl, 0.3M citric acid), 0.1% Tween-20, 50 μg/ml heparin, 9.2mM citric acid and 200 μg/ml yeast tRNA. Once the 2-3 hour pre-hybridization was completed, the solution was replaced with a fresh hybridization solution containing 1ng/μl DIG-labeled antisense RNA probe and the samples were left to hybridize overnight at 70 °C.

At the start of the next day, the samples were kept at 70 °C and transferred to a series of dilutions of hybridization mix and 2x SSC (75% hyb mix:25% 2x SSC, 50% hyb mix:50% 2x SSC, 25% hyb mix:75% 2x SSC and 100% 2x SSC). Once done, the samples were washed for 30 minutes two more times with 0.2x SSC. At this time, the samples were taken out of 70 °C and washed in a series of dilutions of 0.2x SSC and PBST (75% 0.2x SSC:25% PBST, 50% 0.2x SSC:50% PBST, 25% 0.2x SSC:75% PBST and 100% PBST) for 10 minutes each at room temperature. The next step was to pre-incubate the samples for two hours in PBST containing 10% calf serum and 10mg/ml BSA. The following step was an incubation overnight at 4 °C in a solution that contained pre-absorbed anti-DIG antibody conjugated to Alkaline Phosphatase (AP) (Roche).

Pre-absorption of the antibody was performed during the first day of the *in situ* hybridization. About 4-5 spare fins, that were not hybridized, were placed in a solution containing 20µl of calf serum, 20µl BSA and 1µl of anti-DIG AP antibody in 960µl of PBST for 2-4 hours at room temperature and then placed at 4 °C overnight.

At the start of the third day, the samples were quickly washed with PBST and then placed into 6 successive washes in PBST for 15 minutes each at room temperature with gentle shaking. Before performing the chromogenic reaction, the samples were equilibrated in a buffer (100mM Tris pH 9.5, 50mM $MgCl_2$, 100mM NaCl plus 0.1% Tween-20) by washing 3 times for 5 minutes at room temperature. The staining solution was made up of the equilibration buffer in addition to containing 0.175 mg/ml 5-Bromo-4-Chloro-3-Indolyl phosphate (BCIP) and 0.337mg/ml Nitro Blue Tetrazodium (NBT). The samples were placed in the staining solution in the dark at room temperature with gentle shaking until the desired stain color was visualized. At this point, the samples were washed with PBST and post fixed in 4% PFA for two hours before being placed in 100% glycerol for imaging.

2.11 Sectioning of fin samples for *in situ* hybridization

Fins that were fixed in 4% PFA were rehydrated in a series of 5 minutes washes in dilutions of methanol and PBS (75% MeOH: 25% PBS, 50% MeOH: 50% PBS, 25% MeOH: 75% PBS). The samples were then washed three times in PBST for 5 minutes each. Fins were then embedded in a melted embedding gel (1.5% agarose in 1xPBS and 5% sucrose). Once the embedding blocks were solidified, they were trimmed into shape ready for sectioning. The trimmed blocks were then placed in a 30% sucrose in PBS solution and stored at 4°C overnight. The blocks were mounted

on a cryostat chuck perpendicularly in a layer of the cryomatrix (VWR) and then frozen in 2-methyl butane (-80°C). The sectioning was done using a cryostat sectioner (Leica CM3050S) making sections of 16μm thick. Sections were then collected on coated glass slides and stored at –20° until the time of use.

2.12 *In situ* hybridization on cryostat sections

The slides were taken out from the –20°C freezer and thawed at room temperature for at least two hours, then heated up to 60°C for 10 minutes. Slides were then fixed in 4% PFA in PBS, followed by two 5 minute washes in DEPC-PBS (pH7.4). Slides were then incubated for 15 minutes in 0.3% Triton X-100/DEPC-PBS (pH7.4) and washed two times for 5 minutes with DEPC-PBS. The next step was permeabilization treatment with 20μg/ml proteinase K (Invitrogen) for 30 min. Next step was to wash the slides twice for 5 minutes in DEPC-PBS. In the acetylation step I placed the slides in a solution consisting of 500μl triethanolamine and 108μl acetic anhydride in 40ml of DEPC treated water for 5 minutes, and dehydrated in a series of 3-minute washes in dilutions of ethanol and DEPC-treated water (50% ethanol:50% DEPC-H2O, 70% ethanol:30% DEPC-H2O, 95% ethanol:5% DEPC-H2O, 100% ethanol). Next, the slides were pre-hybridized in a solution (50% deionized formamide, 1x NaCl, 10% Dextran Sulfate, 1mg/ml yeast tRNA, 1x Denhardts solution, in DEPC-treated water) at 60°C for 2-3 hours. I pipetted 500μl of the pre-hybridization solution on top of each slide and covered it with a coverslip. The pre-hybridization was done in a sealed plastic box containing a piece of brown paper towel soaked in 0.1xSSC and 50% formamide solution, to create a humidified chamber. The pre-hybridization continued for 2-

3 hours and then the solution was replaced with a fresh pre-hybridization solution containing 1 ng/μl DIG-labelled antisense RNA probe, previously denatured for 5-10 minutes at 70°C. The samples were allowed to hybridize overnight at 60°C.

The next day, the hybridized samples were subjected to several washes at 60°C. The washes were done twice in 2xSSC for 20 minutes, twice in 1xSSC/50% formamide for 20 minutes and twice in 0.2x SSC. This step was followed by two 10-minute washes at room temperature in TBST (0.14M NaCl, 0.27mM KCl, 25mM Tris-HCl and 1% Tween-20). My next step was to pre-incubate the samples for at least 1 hour at room temperature in TBST containing 10% calf serum. The next step was the antibody absorption, which was performed by adding 500μl of 1:2000 anti DIG AP antibody in blocking solution. This step was done overnight in a sealed plastic box containing a piece of brown paper towel soaked in water at 4°C.

On the last day, hybridized samples were put through three washes of 10 minutes each in TBST. Prior to the chromogenic reaction, the fins were equilibrated in 10-minute washes in NTMT equilibration buffer (100mM Tris pH 9.5, 50mM $MgCl_2$, 100mM NaCl). Sections were stained in a solution containing 0.175 mg/ml 5-Bromo-4-Chloro-3-Indolyl phosphate (BCIP) and 0.337mg/ml Nitro Blue Tetrazodium (NBT) in NTMT equilibration buffer at room temperature until a suitable staining color was visualized. After staining, the samples were washed in PBS containing 10mM EDTA and post fixed in 4% PFA for 20 minutes. A quick wash with water preceded the mounting step. Microscopy Aquatex mounting medium was used to mount the slides by placing one to two drops of medium and covering the slide with a coverslip.

2.13 Alcian blue and Alizarin red staining

The first step was to take out fixed fins from the 4% PFA solution and wash them twice in PBS solution for 10 minutes each. My next step was to allow the samples to stain in alcian blue [5mg of alcian blue powder in 50ml of ethanol/acetic acid solution (70% ethanol, 30% acetic acid)] for 6 hours at room temperature. Next step was a dehydration, which involved a series of 30-minute washes in 70% ethanol in PBS, followed by 95% ethanol in PBS, 100% ethanol and then I replaced the 100% ethanol solution and incubated the samples overnight at 4°C.

At the start of the next day, I performed a rehydration step, which involved a series of 50-minute washes in 80% ethanol in PBS, followed by 50% ethanol in PBS, 30% ethanol in PBS and finally in water. I then stained the samples in alizarin red [0.1% of alizarin red in a fresh solution of 0.5KOH (50mg in 10ml of water)] for 4-5 hours at room temperature. I then rinsed the samples in water overnight and prepared them for imaging through a dissecting microscope.

3. Results

3.1 Expression analysis

To begin experiments, I wanted to design RNA probes to allow me to perform the expression analysis using *in situ* hybridization. Initially, I cloned a cDNA fragment for *pthrp1* corresponding to the first 693bp of the coding region using RT-PCR. Also, a 524 bp cDNA fragment for *pthrp2,* a 604bp for *ihha* and a 1980bp fragment for *evx1*. Expression analysis was performed by *in situ* hybridization on whole mount embryos and fins and on fin ray sections. In my analysis of *pthrp1* expression on embryos, there was no discernible pattern of expression that could be detected in my 72hpf embryos (data not shown). A previous group working on *pthrp1 in situ* hybridization on embryos also encountered this difficulty in detecting expression in embryos (Yan et al., 2012). However, Yan and colleagues managed to describe a discernible expression pattern of *pthrp1* in early developing embryos. Their expression of *pthrp1* at 72hpf was detected in the presumptive branchial arches, otic vesicles, pancreas and unidentified regions of the head. This expression pattern is similar to *PTHrP* expression in early developing mouse embryos.

Analysis of *pthrp2* expression in embryos did not yield any discernible staining as well (data not shown). Although difficult to detect, Yan and colleagues also managed to describe *pthrp2* expression at 72hpf to be in a patch of mesenchymal cells of unknown identity and in spinal neuromasts (Yan et al., 2012).

The expression of *pthrp1* in fin regenerates was analyzed using *in situ* hybridization on whole mount and longitudinal sections. Expression of *pthrp1* as visualized by the staining on whole mount specimens of fin regenerates was prominent in a distinct group of cells in the distal portion

of newly regenerating fin rays, forming a horizontal line across each fin ray (Figure 3.1AB). Time course analysis showed that the pattern of expression is visible starting at 2dpa to 6dpa (last time point tested). At 1dpa, the regenerate is minimal so it was very difficult to detect expression by *in situ* hybridization (data not shown). There was no staining detected for *pthrp2* using *in situ* hybridization on fin regenerates. The *in situ* hybridization experiment was performed at least three times with a minimum of seven whole fin tissue samples for each probe. The *pthrp1* pattern of expression was visible in each hemiray, such that two distinct, horizontal lines of cells expressing *pthrp1* are present on opposite sides of the whole mount fin. However, some fin rays did not show any expression of *pthrp1* (Figure 3.1F), while other fin rays on the same fin showed expression. In certain cases within a single fin ray expression was seen in one hemiray (partial expression, Figure 3.1A green box).

Although not as prominent, there was a visible staining in the area of newly formed and forming joints/segment boundaries (Figure 3.1A black arrow, Figure 3.2A red arrows). This staining was usually faint, but it was always associated with joints and it appeared as small patches of staining. I also observed that the horizontal line domain of expression splits into two smaller lines in fin rays that were about to undergo bifurcation. By changing the lighting and the focus on the image, this became visible on the left domain of expression in the representative whole mount image (Figure 3.1B).

To have more precise information regarding the cell types expressing *pthrp1, in situ* hybridization was performed on longitudinal sections of fin regenerates. The expression was restricted to a select group of cells, almost like a small circle, localized in the blastema and lining the basal epidermis (Figure 3.1C, white arrows, Figure 3.2A). The expression domain of *pthrp1* was within the described domain of *ihha* in the differentiating osteoblasts, shown previously by

Avaron and colleagues (Figure 3.1D & E, black arrows) (Avaron et al., 2006). However, the expression pattern of *pthrp1* was localized to a single subset of these cells, while the expression pattern of *ihha* was more extended along the longitudinal axis of the fin ray.

Leona Probst, in our lab, previously showed by *in situ* hybridization on whole-mount fins, that *evx1* is expressed in a similar domain of expression as *pthrp1*. The expression pattern of *evx1* and *pthrp1* was compared by *in situ* hybridization on consecutive sections of fin regenerates. *Evx1* expression on sections showed an identical pattern to that of *pthrp1* (Figure 3.2B, C, D and E). We also performed double *in situ* hybridization for both *pthrp1* and *evx1* and there was an overlap in the expression profile (Data not shown). In embryos, there was a distinct expression pattern for *evx1* seen through *in situ* hybridization at 2dpf, 3dpf and 4dpf, which was concentrated in the head region at the central nervous system (Figure 3.2F). The expression of *evx1* in embryos was found in the nervous system, neural tube, cerebellum and other brain regions.

Finally, I was not successful in detecting expression of *ihha* using *in situ* hybridization in both embryos 3dpf, 4dpf and 6dpf and fins at 3dpa and 4dpa. During those experiments, my control probes, which were *pthrp1* and *evx1*, gave me the expected expression under the same conditions as *ihha* probe and at the same time points.

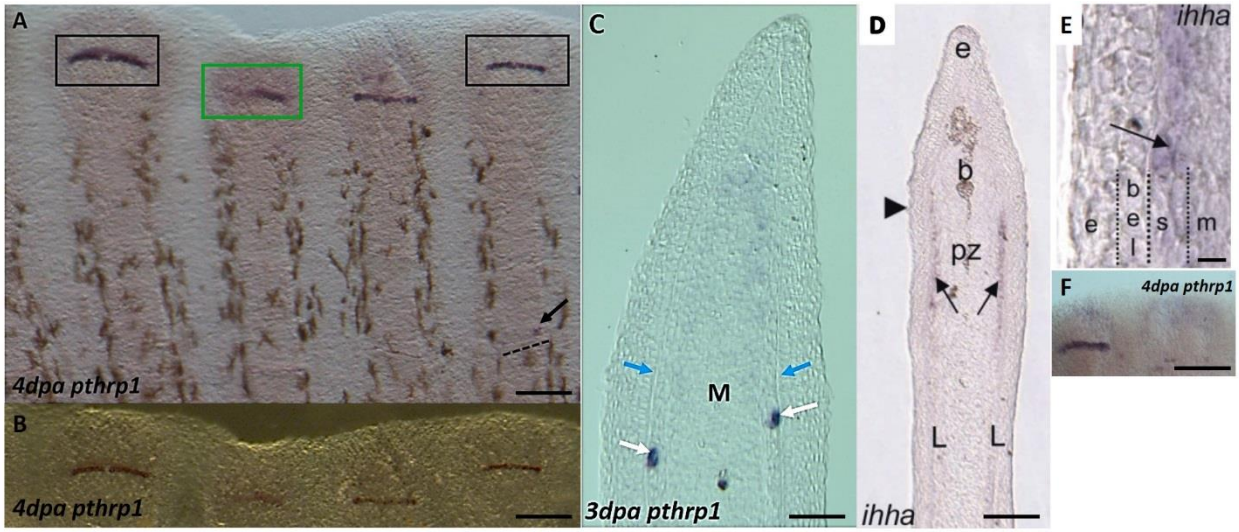
A
4dpa pthrp1
B
4dpa pthrp1
C
M
3dpa pthrp1
D
e
b
pz
L
L
ihha
E
ihha
e
b
e
l
s
m
F
4dpa pthrp1

Figure 3.1. Expression pattern of *pthrp1* on whole-mount fin regenerates and regenerate sections and expression pattern of *ihha* on section by *in situ* hybridization. (**A**) *pthrp1 in situ* hybridization on a whole mount regenerating zebrafish caudal fin at 4dpa. The horizontal line of cells depicts the most prominent expression of *pthrp1* in regenerating fins in a subset of blastema cells (newly differentiating osteoblasts) (black box). In some of the samples, there is faint expression (black arrow) associated with the position of already formed joints (right above dashed line). (**B**) Same image as **A**, but different lighting showing how the expression domain divides into two before the ray bifurcation occurs (left ray) (**C**) *pthrp1 in situ* hybridization on sections of a single zebrafish caudal fin ray. The expression of *pthrp1* on section is visible by the blue staining (white arrows) and it is present in a subset of the newly differentiating osteoblast cells just inside bony rays (blue arrows) but not too deep into the mesenchyme (M). (**D**) *ihha in situ* hybridization on longitudinal sections showing the expression domain (black arrows) in newly differentiated osteoblasts along the fin ray just inside the newly formed lepidotrichia (L). Proliferation zone (pz), epidermis (e) and blastema (b) are labeled as well. (**E**) A magnification of the expression pattern of *ihha* (black arrow) where we see the expressing osteoblasts (s) are just inside the bone and basal epidermal layer (bel) and epidermis (e), but not as deep as the mesenchyme (m). (**F**) A sample *in situ* hybridization image showing that the expression pattern of *pthrp1* is not always consistent and here we see that one ray has expression and the other adjacent does not. Scale bar in A and B: 2 mm, on C: 0.15 mm, on D: 0.3 mm, on E: 0.08 mm and on F: 1 mm. Both panel **D** and **E** are adapted from Avaron and colleagues with permission (Avaron et al., 2006).

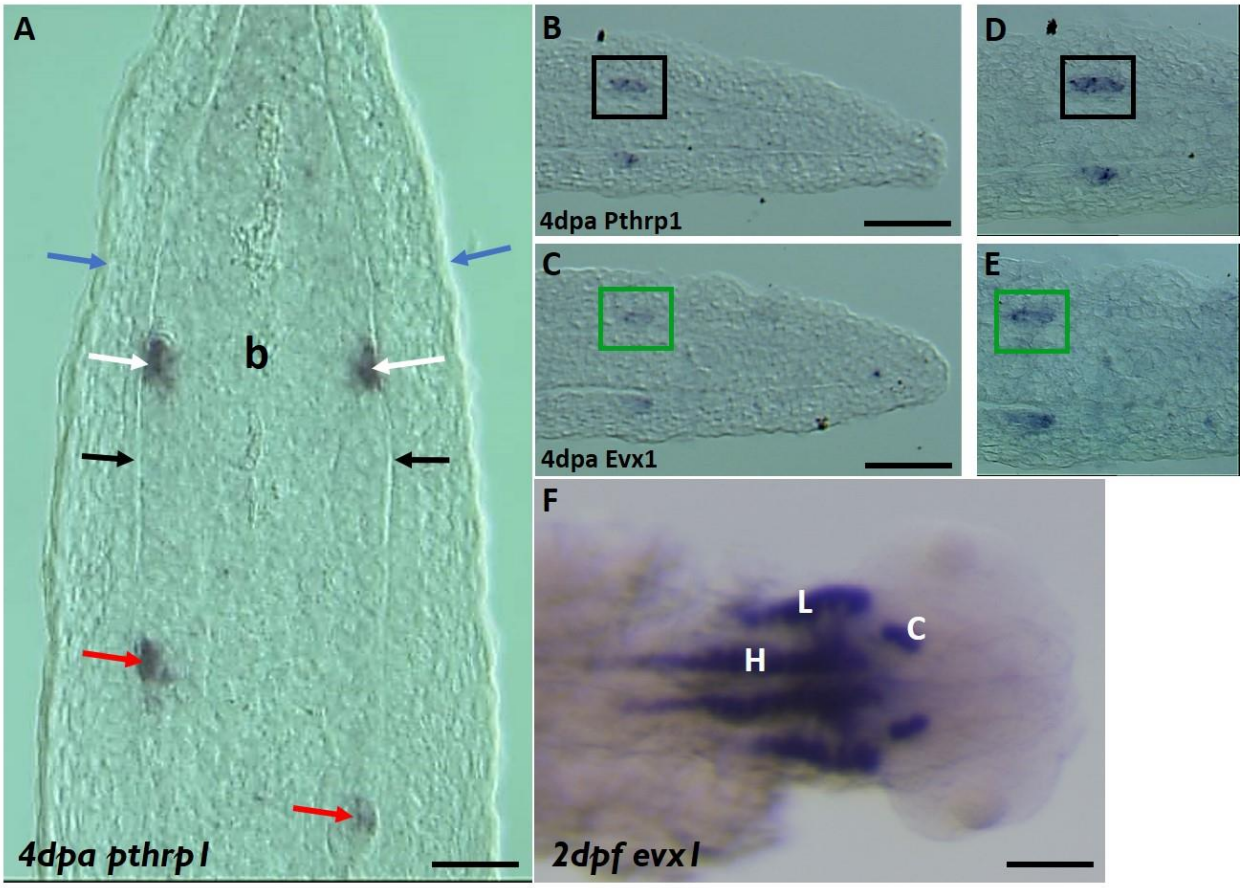
A
b
4dpa pthrp l
B
4dpa Pthrp1
D
C
4dpa Evx1
E
F
L
C
H
2dpf evx l

Figure 3.2. Expression analysis of *pthrp1* on longitudinal fin sections with a comparison to the expression of *evx1* using *in situ* hybridization. The same expression as in Figure 3.1, but seen on sections (**A**) Expression domain of *pthrp1* as seen by *in situ* hybridization on a longitudinal section of a single 4dpa regenerating fin ray. The typical expression pattern in the distal region is visible in the image (white arrows), but there is another domain of expression (red arrows), which matches the faint expression seen in the whole mount *in situ* hybridization at the level of the joints. This expression pattern is not always visible but it is mostly localized at the level of newly formed joints. The epidermis is shown with blue arrows, ossified bone in black arrows and the blastema labeled b. (**B, C**) The expression pattern of *pthrp1* at the level of newly forming joints (black box in B) was compared to the expression of *evx1* (green box in C), which we knew was expressed at segment boundaries (both at 4dpa). There was a clear co-localization between the expression domains of the two genes as seen in the magnified images (**D, E**). (**F**) Expression pattern of *evx1* in 2dpf embryo using *in situ* hybridization showing the cerebellum (C), lateral sensory area of brain (L) and hind brain medial neurons (H). Scale bar in A: 0.27 mm, in B and C: 0.2 mm and in F: 0.3 mm.

3.2 Morpholino knockdown

In order to expand my understanding of the roles played by Pthrp1 and Ihha, I decided to perform a knockdown of these genes using *in vivo* electroporation of morpholinos in regenerating caudal fins. Morpholinos are antisense to their target mRNA and they block access of other molecules to the mRNA, which will render it inactive and hence knock down the gene of interest. The morpholinos can be labeled with a fluorescein tag, which helps in the tracking of the maintenance and the stability of the morpholino over time (Kos *et al.*, 2001). Both of the morpholinos for *pthrp1* and *ihha* were translation-blocking morpholinos, which means that they are designed to bind around the translation initiation codon and prevent translation of the targeted transcript.

The method of injection was obtained from published protocols for *in vivo* electroporation of morpholinos in zebrafish, mostly from Thummel and colleagues (Thummel *et al.*, 2006). The details of the injection protocol can be found in the "Materials and Methods" section. 90 nl of 1mM morpholino was directly injected into the blastema of regenerating fin rays at 2dpa and injection was directly followed by electroporation (Figure 3.3). Injection was performed in the five outer fin rays (long rays), but excluding the outer most rays. The electroporation was done using ECM 830 Square Wave Electroporator (BTX Harvard Apparatus) and the parameters used were 15 consecutive 50-msec pulses, at 15 V with a 1-sec pause between pulses.

3.2.1 Control morpholino test

The first morpholino injection was made using control morpholinos that are made up of a random sequence and that are not meant to produce any effect. I wanted to observe if the injection

on its own is responsible for any negative effects on regeneration compared to un-injected fins and to optimize the injection parameters. Standard control morpholino (containing a 3' fluorescein tag from Gene Tools, LLC) was injected on both lobes of the fin. Fin rays of regenerating fins at 3dpa of a minimum of 10 fish were injected with control morpholino in three independent experiments. At 24 hours post injection (hpi), morpholino oligonucleotides were distributed uniformly in cells across the blastema, as detected by green fluorescence, which suggests that the injection was efficient and of good quality (Figure 3.4). Fluorescence was detected only in injected regions in the wound epidermis and essentially in the blastema. In this control test, no morphological defects in comparison to wild type un-injected fins were observed between 1dpi and 4dpi (Figure 3.5). The morpholino injected fins in this figure were presented under different brightness to clearly show the bones and joints showing no deformity during regeneration.

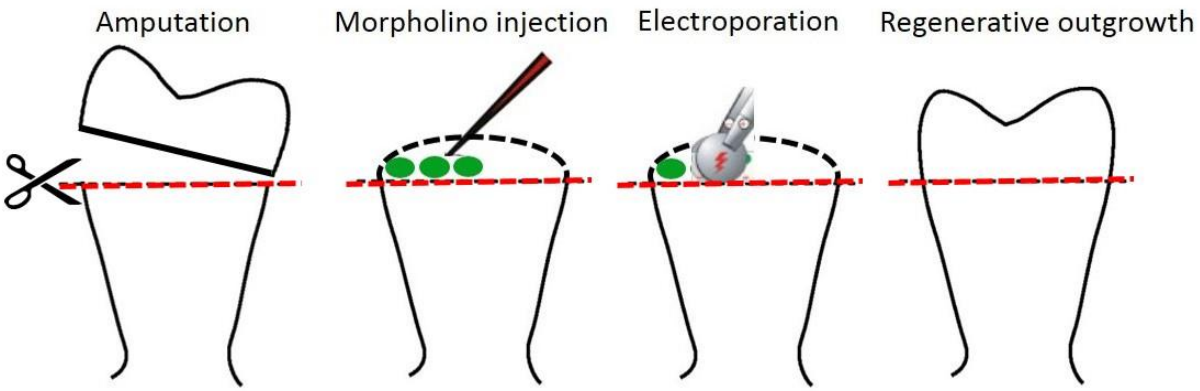
Amputation
Morpholino injection
Electroporation
Regenerative outgrowth

Figure 3.3. Schematic showing the method of *in vivo* injection and electroporation. The first step is amputation at the same level across the entire fin marking hour 0 of the experiment (0hpa). The second step is the microinjection of the morpholino of interest (green circles) in the blastema of regenerating fin rays at 48hpa. Immediately following injection, the dorsal (experimental side) and the ventral (control) side are electroporated using plate tweezertrodes. At 72hpa, observations of the regenerative outgrowth begins. Red dashed line represents the plane of amputation.

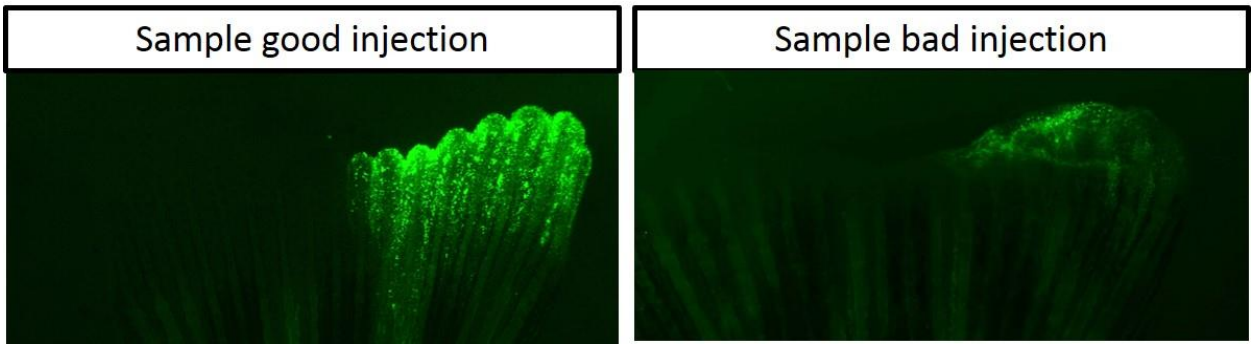
Sample good injection
Sample bad injection

Figure 3.4. Sample images representing an injection of good quality on the left versus one of poor quality on the right. The good quality injection shows a uniform distribution of fluorescence in the injected areas of the regenerating fins. In poor quality injections, the fluorescence is either concentrated in small area as seen in sample image on right or distributed throughout the whole fin with no specificity. These observations were done at 2dpi. Images show the injection of the dorsal side.

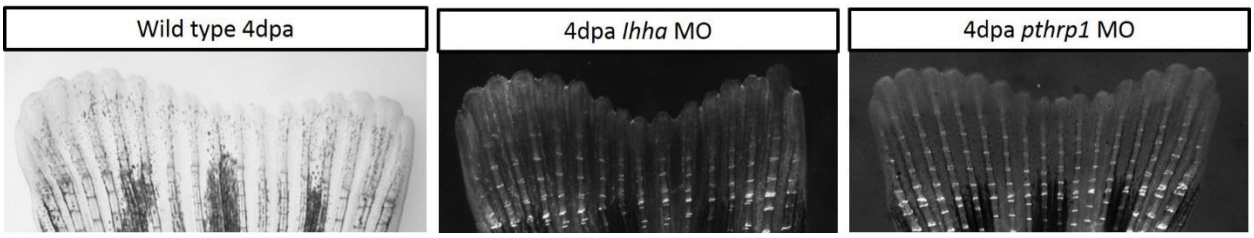
Wild type 4dpa
4dpa *Ihha* MO
4dpa *pthrp1* MO

Figure 3.5. Comparative figure showing the regeneration process of a wild type intact fin alongside fins injected with morpholino for *pthrp1* and *ihha*. There were no morphological defects to be reported. Morpholino was injected on the dorsal side of the fin (right side in all images).

I then moved on to perform the experimental morpholino knockdown experiments. There were no observable toxic effects associated with the morpholinos as all the injected fish survived with no visible problems. The day after injection, the quality of the injection was assessed based on the localization of the fluorescence within each blastema. Once fish with injections of good quality were chosen, they were analyzed morphologically for differences between the experimental and control sides. I was looking for any physical deformities in the regenerating bones using a dissecting microscope. In addition, measurements of fin ray growth and of the area of the regenerative outgrowth were performed. Finally, the regenerating bones were stained using alcian blue and alizarin red stain to visualize the extent of ossification.

3.2.2 Fin ray length analysis

In the *pthrp1* MO-injected fins, there was no visible deformity or difference in the morphology of the bones in the lobe injected with *pthrp1* morpholino and the lobe injected with standard control morpholino within the same fin. A total of 37 adult fish were injected and about 30 fish were classified as injections of good quality throughout three trials (10 fish in each trial). No morphological defects were detected under a dissecting microscope between 1dpi and 4dpi (Figure 3.5). Next, Using ImageJ Software (Image processing and analysis in Java, version 1.46), the length of each fin ray was measured starting from the amputation line to the tip of the regenerate, at 4 days post injection (dpi), which means 6dpa. These measurements were performed for the four outer long rays because they grow the fastest excluding the outer most rays (Figure 3.6A). The length of each ray on the experimental side was compared to the corresponding ray on the control side. On average, under normal conditions, the growth is greatest in outer most ray number 1 and, as one moves towards the center of the fin, the growth rate is less. There was no significant difference in the growth of the outer four fin rays of the regenerate between morpholino-injected

rays and control-injected rays (Figure 3.6B). The statistical analysis was done using t-test for each fin ray with a p-value of 0.33, 0.32, 0.34 and 0.36 for fin rays 1-4 respectively.

In the *ihha* MO-injected fins, similar to the *pthrp1* MO results, there was no visible deformity or difference in the morphology of the bones in the experimental side versus the control side (Figure 3.5). A total of 42 adult fish were injected and about 35 fish were classified as injections of good quality throughout three trials (10 fish in two trials and 15 in last trial). At 4dpi, the measurements showed no significant change in the growth rate of the fin rays injected with experimental morpholino (Figure 3.6B). The statistical analysis was done using t-test for each fin ray with a p-value of 0.21, 0.27, 0.31 and 0.29 for fin rays 1-4 respectively.

A

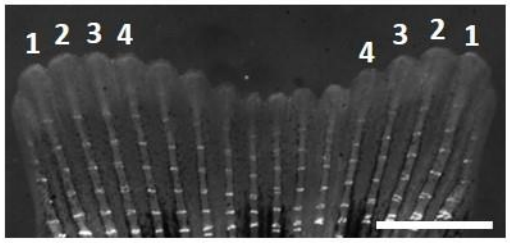
1 2 3 4
4 3 2 1

B

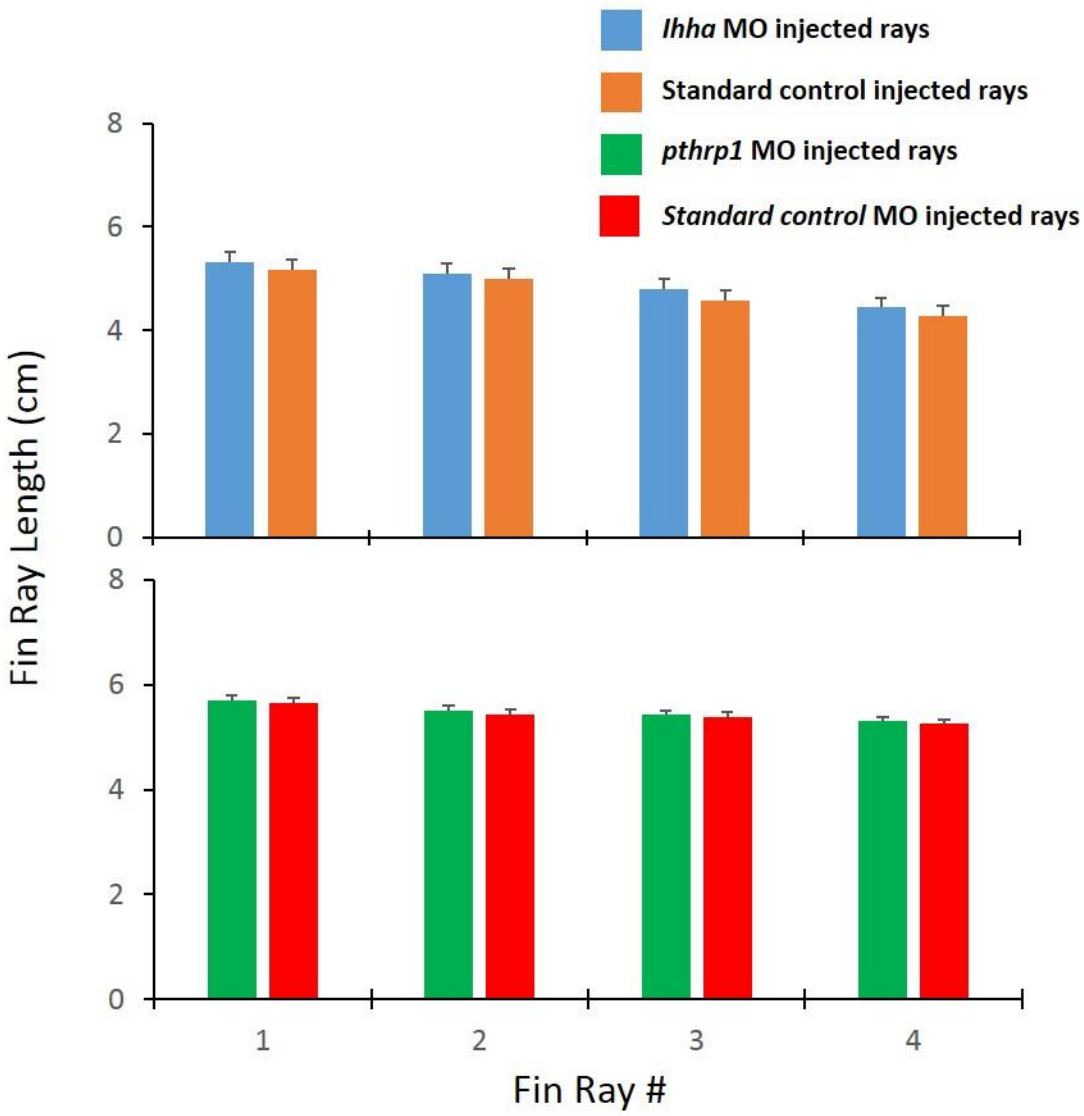
Ihha MO injected rays
Standard control injected rays
pthrp1 MO injected rays
Standard control MO injected rays
Fin Ray Length (cm)
0
2
4
6
8
1
2
3
4
Fin Ray #

Figure 3.6. Illustration showing the injected fin rays and a graph comparison between the ray lengths from morpholino and control injected lobes. (**A**) The measurements of length were done on injected fin regenerates from the amputation line to the tip of each ray for the outer four rays at 4dpi/6dpa. (**B**) Two panel graph representing a comparison between the length of the outer four rays of the caudal fin in response to a targeted morpholino injection or a standard control injection. The upper panel represents *ihha* MO injection and the lower panel represents *pthrp1* MO injection. Both panels have a standard control morpholino injection. On the X-axis we have the ray number as per the explanatory image (A). Scale bar in A: 0.16 cm.

3.2.3 Bone Staining

In light of the results that showed no change in the fin ray growth despite the knock down of *pthrp1* and *ihha*, I decided to look directly at the level of bone ossification. Since I have discussed the important roles PTHrP and IHH play in bone formation, I wanted to observe the ossification front by alizarin red staining. At the same time, I performed Alcian blue staining, a marker for glycosaminoglycans abundant in the undifferentiated bone matrix of the fin rays (Smith et al., 2006).

I analyzed the ossification of the bones in the regenerate after the injection of *pthrp1* and *ihha* morpholinos into fin regenerates. I used the same fins that I analyzed for the growth in fin ray length earlier. The bone staining was done on fin regenerates that were injected and then amputated and fixed for staining at 5dpi (7dpa). Alizarin red stained ossified bone red, which was clearly visible under a dissecting microscope equipped with a color camera. In both *pthrp1* and *ihha* MO-injected fins, there was no discernible change in bone ossification (Figure 3.7).

In terms of the Alcian blue staining, there was no clear blue staining detected in the fin regenerates. Only some small patches of blue staining were observed mostly at the tip of the regenerating fin rays (Data not shown). These patches seen at the distal ends are glycosaminoglycans present there because dermal bones are still being formed. Cartilage specific markers have been shown to be expressed in cells that will secrete a matrix that will form dermal bone (Smith et al., 2006).

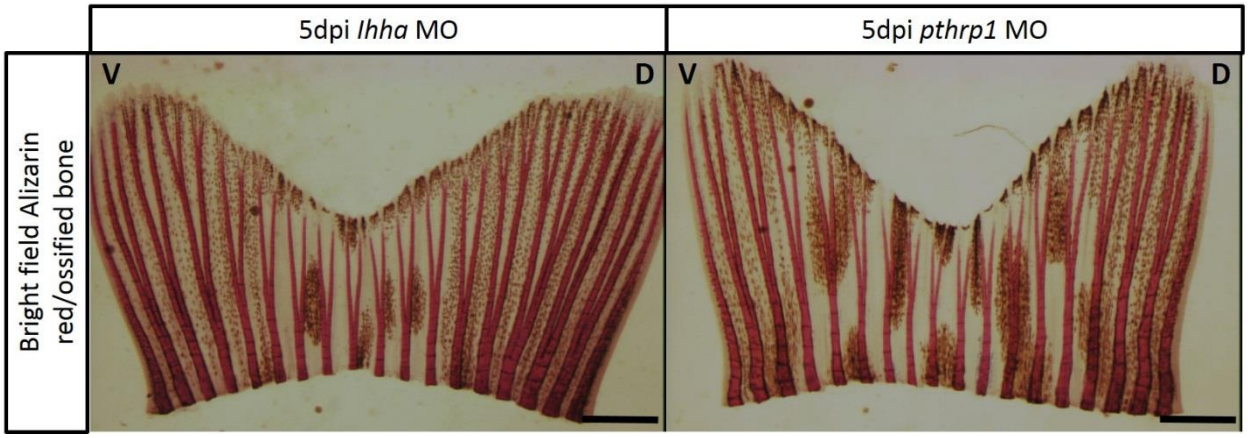
5dpi *Ihha* MO
5dpi *pthrp1* MO
Bright field Alizarin red/ossified bone
V
D
V
D

Figure 3.7. Representative whole mount fins showing the ossification of bones by alizarin red and alcian blue staining at 5dpi/7dpa from *ihha* or *pthrp1* MO-injected fins. Alizarin red stains ossified bone. The *ihha* and *pthrp1* morpholinos are both injected on the dorsal side (D) of their respective image and the ventral side (V) is injected with standard control morpholino. Scale bar is approximately 0.09 cm.

3.2.4 Regenerative outgrowth area analysis

I decided to change the time of observation in the next set of morpholino injections. I observed my samples at 2dpi instead of 4dpi because it seems that the 4dpi time point gives enough time for the morpholino-injected side to recover in growth with the control side. Another difference here was that I changed my method of injection; I divided my fish into groups, and only injected the dorsal lobe of each caudal fin. One group was injected with *pthrp1* morpholino into the dorsal lobe while the ventral lobe was left intact (Figure 3.8). In this experiment, I analyzed the fin ray length and the area of regenerative outgrowth between morpholino-injected experimental lobe and uninjected control lobe. The same injection method was used for the second group, but I used standard control morpholino for the dorsal lobe instead. A total of 10 fish were analyzed for the standard control injection and 10 fish for the *pthrp1* MO-injection. At 2dpi (4dpa), the length of fin rays was measured and compared between injected rays and intact rays on opposite lobes. The group injected with standard control morpholino showed no significant difference between the injected lobe and the intact lobe (Data not shown). The group injected with *pthrp1* experimental morpholino showed a significant difference in fin ray length between injected rays on one lobe and intact un-injected rays on opposite lobe (Figure 3.9). In addition, ImageJ software was used to outline the area covered by the four injected experimental rays and their corresponding un-injected control rays (Figure 3.10A). An outline was drawn around the outer four long rays, with the base of the outline being the amputation line and the top being the tip of the outgrowth (Figure 3.10B). Using ImageJ software, I computed the values corresponding to the area covered by the outline and hence was able to compare the changes in outgrowth between the injected fin lobe and the un-injected lobe (Figure 3.10C). In fish that were injected with standard control, there was no significant difference in the regenerative outgrowth between the two lobes (Figure 3.11A).

Statistical analysis was done using a t-test and the p-value was 0.39. When comparing my experimental *pthrp1* experimental morpholino injected group to the standard control group, the area of regenerative outgrowth after injection showed a significant difference between the two lobes of the caudal fin (Figure 3.11B). Statistical analysis was done using a t-test and the p-value was 0.04. In *pthrp1* morpholino group, the area of the regenerative outgrowth of the injected lobe was smaller than the area of the un-injected lobe. This can be compared to the control group, where the area of regenerative outgrowth changed very little or did not change at all between the two lobes of the caudal fin (Figure 3.11A). Therefore, the standard control morpholino did not inhibit regenerative outgrowth, but the *pthrp1* morpholino inhibited regenerative outgrowth by 10-15% (Figure 3.11B; $P < 0.04$).

Here I also reassessed the fin regeneration response using *ihha* morpholino injections. Again, I performed the injection of *ihha* morpholino on the dorsal lobe of the fin and left the other lobe intact (Figure 3.8). I analyzed a total of 10 fish for *ihha* injections. As in the *pthrp1* group, I measured the fin ray length and there was a significant difference in the length of rays that were injected with *ihha* morpholino in dorsal lobe versus those uninjected intact rays in ventral lobe (Figure 3.9). I also measured the area of the regenerative outgrowth in the *ihha* morpholino injected lobe in comparison to the un-injected control lobe. The measurements were performed by following the same procedure used for the *pthrp1* MO-injection. The growth of the regenerate in the injected lobe at 4dpa was less than the growth in the un-injected lobe, as shown by the area measurements (Figure 3.11B). *ihha* morpholino inhibited regenerative outgrowth by 25-30% on the dorsal lobe in comparison to the intact ventral lobe (Figure 3.11B; $P < 0.03$).

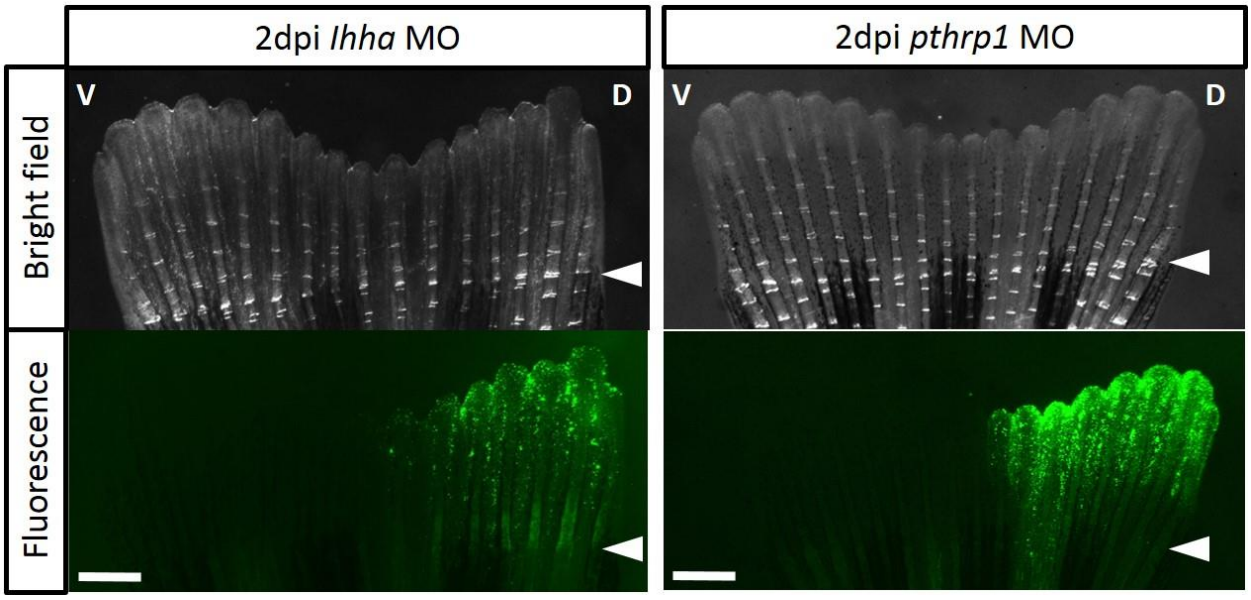
2dpi *Ihha* MO
2dpi *pthrp1* MO
Bright field
Fluorescence
V
D
V
D

Figure 3.8. Representative images showing bright field and fluorescence images of *ihha* or *pthrp1* morpholino injections on the dorsal lobe of the regenerating caudal fin rays at 2dpi/4dpa. These images are also representative of good quality injections. White arrowheads represent the amputation line, dorsal lobe (D) and ventral lobe (V). Morpholino was injected on the dorsal lobe. The scale bars = 0.075 cm.

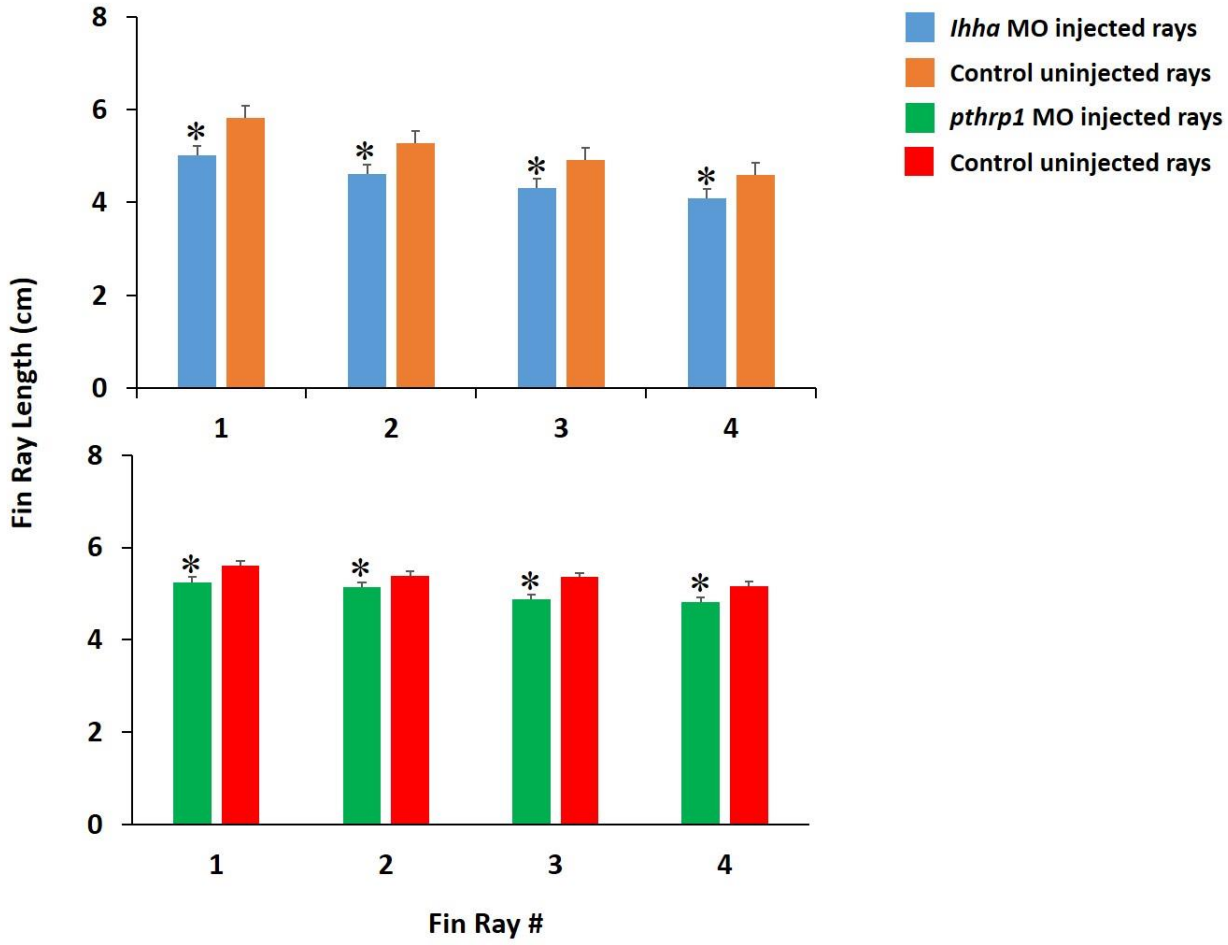
Ihha MO injected rays
Control uninjected rays
pthrp1 MO injected rays
Control uninjected rays
Fin Ray Length (cm)
0
2
4
6
8
1
2
3
4
Fin Ray #

Figure 3.9. A graph comparison between the ray lengths from experimental morpholino injected lobes and control uninjected lobes using the second method of analysis. Two panel graph representing the comparison between the lengths of the outer four rays of the caudal fin in response to an experimental morpholino injection versus intact uninjected rays. The upper panel represents *ihha* MO injection and the lower panel represents *pthrp1* MO injection. The measurements of length were done on regenerating fin rays from the amputation line to the tip of each ray for the outer four rays at 2dpi/4dpa. There was a significant difference in the fin length between all the experimental morpholino injected fin rays and the uninjected control fin rays. In the *ihha* morpholino injection, the p-values for the difference were 0.039, 0.038, 0.04 and 0.043 for fin rays 1-4 respectively. In the *pthrp1* injections, the p-values were 0.042, 0.044, 0.037, 0.04 for fin rays 1-4 respectively.

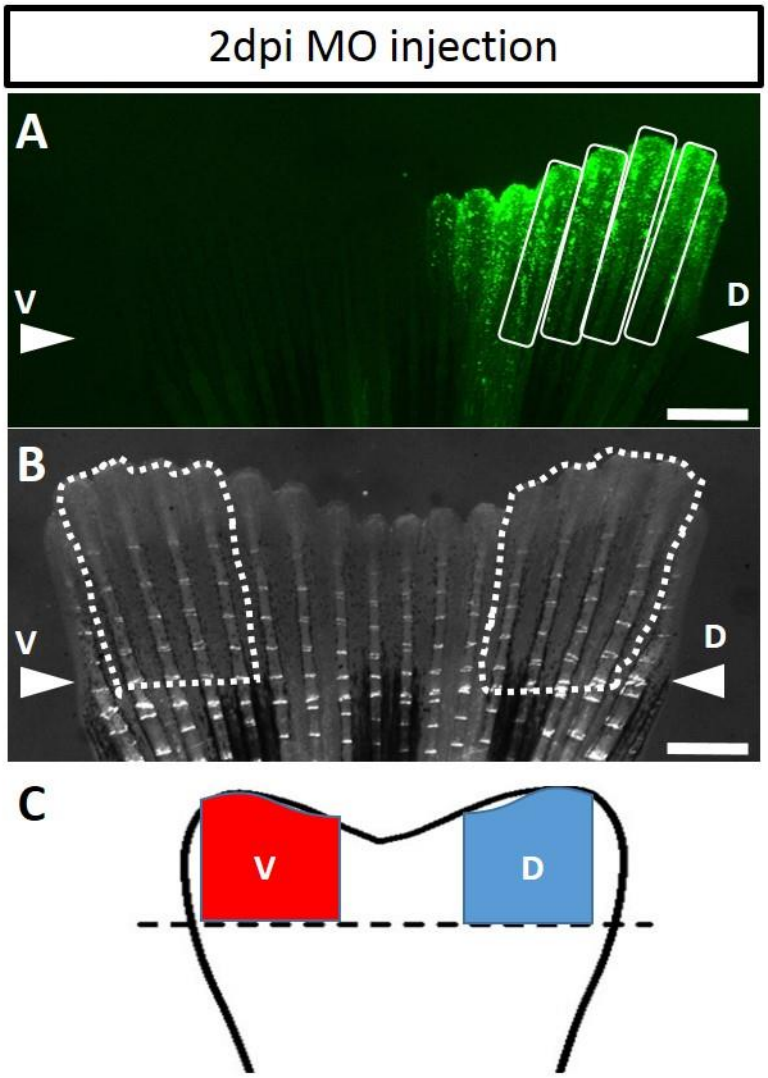

$$\%\ Difference = \frac{Dorsal\ injected\ area\ (D)}{Ventral\ control\ area\ (V)} \times 100\%$$

Figure 3.10. Illustration showing the method used to specify and measure the area of regenerative outgrowth. (**A**) Representative fluorescence image of *pthrp1* morpholino-injected caudal fin rays at 2dpi/4dpa only in the dorsal lobe, showing the outer four fin rays having good distribution of morpholino enclosed in white rectangles. (**B**) Representative bright field image showing *pthrp1* morpholino-injected caudal fin rays with the area to be measured (between rays from image A) enclosed within the dashed white line on the dorsal and ventral lobes of the fin. (**C**) Fin schematic showing the areas we measured from the dorsal and the ventral lobes of the fin. White arrowheads shows the amputation plane, dorsal side (D) and ventral side (V). Scale bars = 0.07 cm.

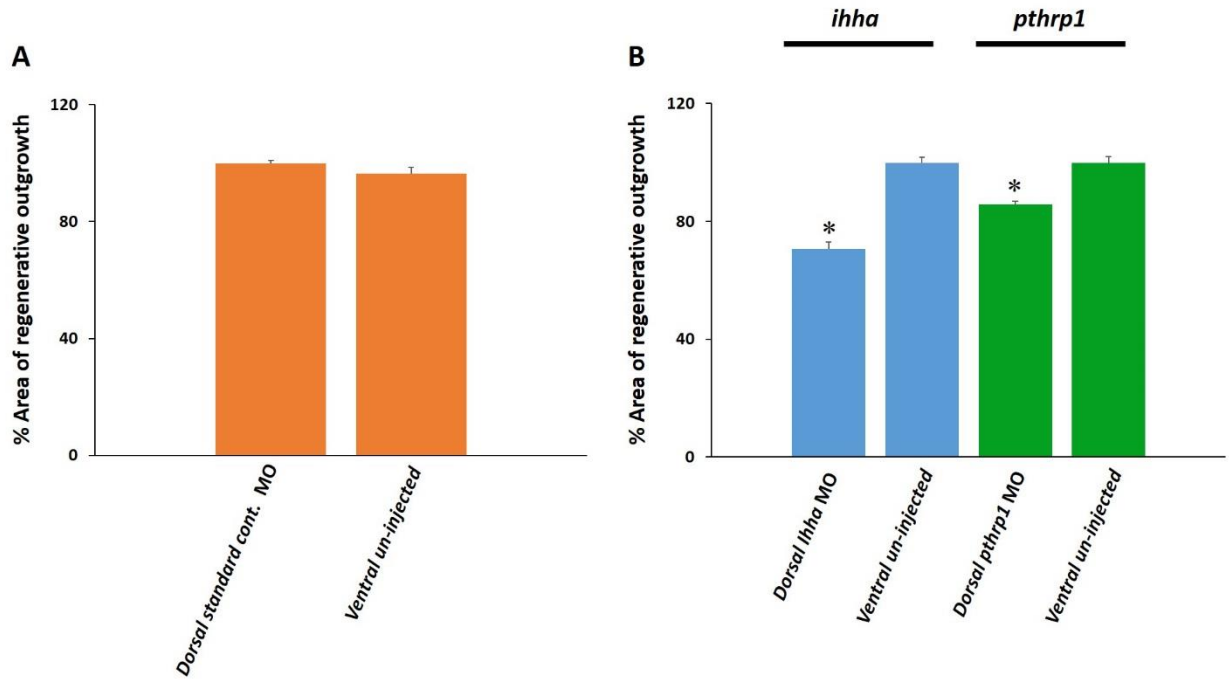
A
% Area of regenerative outgrowth
120
80
40
0
Dorsal standard cont. MO
Ventral un-injected
B
ihha
pthrp1
% Area of regenerative outgrowth
120
80
40
0
*
*
Dorsal Ihha MO
Ventral un-injected
Dorsal pthrp1 MO
Ventral un-injected

Figure 3.11. (**A**) Graph comparing the percentage of area of the regenerative outgrowth in response to the injection of standard control morpholino (orange bars) in the experimental (dorsal) lobe versus the growth of the un-injected control (ventral) lobe. These measurements were done at 2dpi/4dpa. (**B**) Graph comparing the percentage of area of the regenerative outgrowth of the experimental (dorsal) lobe and the control (ventral) lobe for the *ihha* and *pthrp1* groups of morpholino injections. The blue bars represent the *ihha* morpholino injected group and the green bars represent the *pthrp1* morpholino injected group. The asterisks in B denotes a significant difference in the regenerative outgrowth between the injected dorsal lobe and the un-injected ventral lobe (*ihha* group $P < 0.03$ and *pthrp1* group $P < 0.04$).

3.3 RT-PCR Analysis

Since I knew that the second gene, *pthrp2,* of the *pthrp gene*-family was expressed during zebrafish embryo development, I decided to perform RT-PCR experiment to determine if *pthrp2* and *pthrp* receptors are expressed during fin regeneration. The small degree of inhibition seen in my morpholino injections led me to question whether Pthrp2 has a role during regeneration. It has been reported that duplicate genes play redundant or compensatory roles (Gu et al., 2003), which led me to analyze if *pthrp2* is expressed in fin regenerates. I tested the receptors as well to determine which receptor is involved in the regenerate. I made cDNA from RNA, which I collected from 4dpf whole embryos and 4dpa fin regenerates. I then performed a reverse transcriptase PCR analysis using the cDNA. I used this developmental stage for embryos because I know that the genes are expressed at 3dpf and 4dpf (Yan et al., 2012). Moreover, in the regenerates, my previous analysis has shown that *pthrp1* is expressed as early as 48hpa and up to 6dpa. Therefore, I decided to use 4dpa as my time point for RT-PCR analysis. To extract about 20µl of RNA I used 30-50 embryos and about 10 fin regenerates.

I performed a minimum of three trials for RT-PCR analysis for each set of primers. I was unable to show the expression profile of all gene fragments amplified all together simultaneously, since each set of primers was optimized to amplify at a different temperature. My analysis showed that *pthrp2*; is expressed in both embryos and fins at 4dpf and 4dpa respectively (Figure 3.12A). In addition, the PCR analysis for the receptors of the *pthrp* family showed that *pth1r* and *pth2r* are expressed in the 4dpf embryos and 4dpa fin regenerates. The third receptor *pth3r* was expressed in 4dpa fins, but it was not detected in 4dpf embryos (Figure 3.12B). The RT-PCR products for *pthrp1*, *pthrp2*, *pth1r* and *pth2r* were purified and sequenced. The sequences corresponded to the

sequences of *pthrp1*, *pthrp2*, *pth1r* and *pth2r* corresponding zebrafish sequence database (Ensembl). For quantification, I normalized the starting cDNA by measuring the exact concentration for my cDNA and using the same amount for each PCR. It was found that the intensity was almost identical between *pthrp1* and *pthrp2* in both 4dpf embryos and 4dpa fins (Data not shown). This put me in a position to question the role of *pthrp2* since it is possibly being expressed in the fins to a similar level as *pthrp1*.

Reverse transcriptase PCR analysis using cDNA from *evx1* homozygous mutant fins and primers for *pthrp1* and *pthrp2* was done to determine if these genes are expressed in fins that lack joint/segment boundaries. I observed that both genes were expressed in the *evx1* mutants' fin regenerates (Figure 3.13), which is similar to what was observed in the wild type fin regenerates.

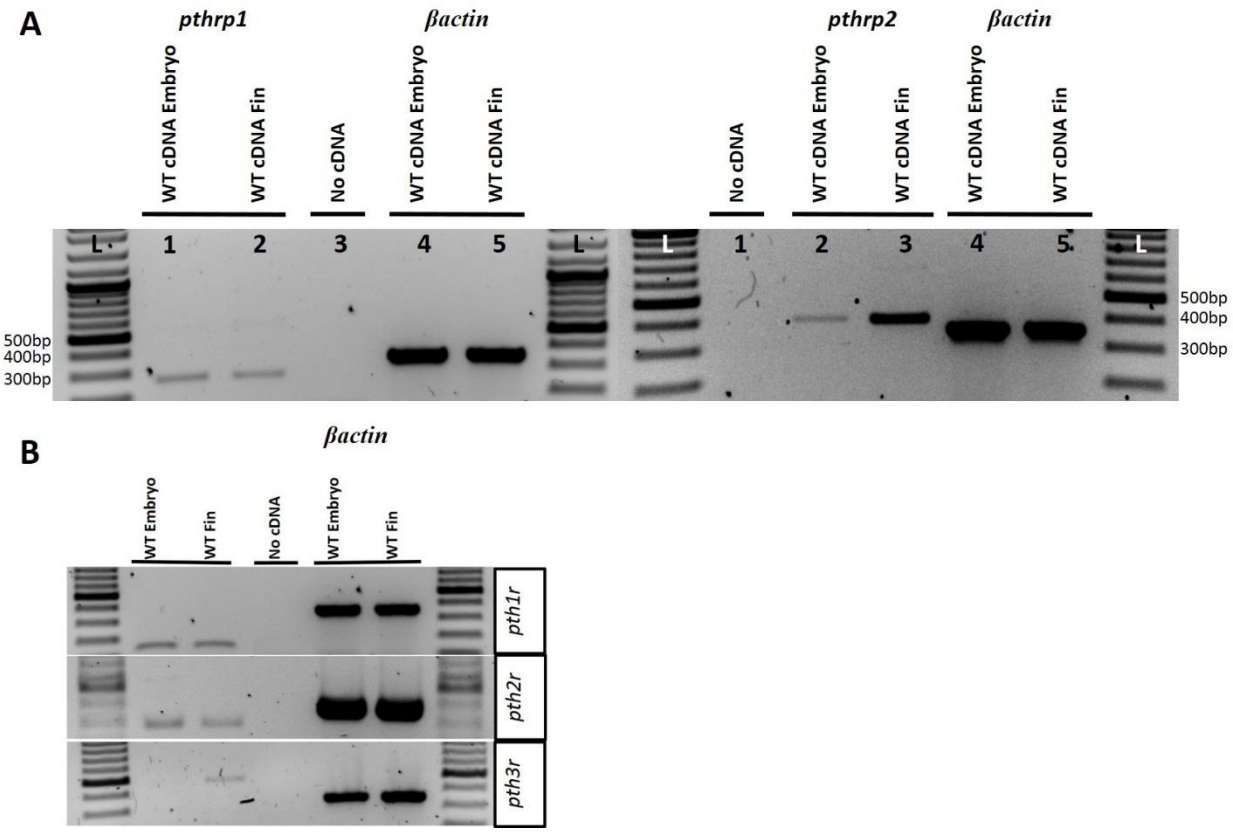
A
pthrp1
βactin
pthrp2
βactin
WT cDNA Embryo
WT cDNA Fin
No cDNA
WT cDNA Embryo
WT cDNA Fin
No cDNA
WT cDNA Embryo
WT cDNA Fin
WT cDNA Embryo
WT cDNA Fin
L
1
2
3
4
5
L
L
1
2
3
4
5
L
500bp
400bp
300bp
500bp
400bp
300bp
B
βactin
WT Embryo
WT Fin
No cDNA
WT Embryo
WT Fin
pth1r
pth2r
pth3r

Figure 3.12. RT-PCR analysis of the expression of *pthrp* gene family and their receptors. (**A**) Expression of *pthrp1* and *pthrp2* in cDNA from 4dpf embryos and in cDNA from 4dpa fin regenerates. (**B**) Expression of the three *pthrp* receptors in zebrafish using 4dpf embryo cDNA and 4dpa fin regenerate cDNA. My positive control was β-*actin* and the negative control contained no cDNA.

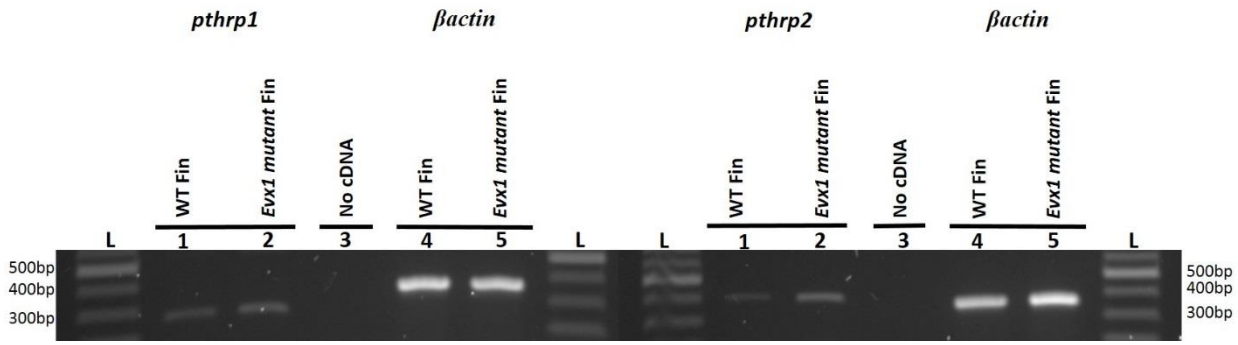
pthrp1
βactin
pthrp2
βactin
WT Fin
Evx1 mutant Fin
No cDNA
WT Fin
Evx1 mutant Fin
WT Fin
Evx1 mutant Fin
No cDNA
WT Fin
Evx1 mutant Fin
L
1
2
3
4
5
L
L
1
2
3
4
5
L
500bp
400bp
300bp
500bp
400bp
300bp

Figure 3.13. RT-PCR analysis of the expression of *pthrp1* and *pthrp2* in the fin regenerates of zebrafish *evx1* homozygous mutants. We used 4dpa fin regenerates from wild type fish and regenerates from *evx1* mutants' fins for the mRNA collection and analysis of expression. My positive control was β-*actin* and the negative control contained no cDNA. 35 cycles of amplification were performed for each PCR.

4. Discussion

The capacity for regeneration in zebrafish is an intriguing phenomenon, which is very important to understand because it has many possible implications. One such implication is the application of this phenomenon into the regenerative medicine field in human beings. The caudal fin is one of the structures that are extensively studied to help dissect the molecular pathways of epimorphic regeneration especially the regeneration of bones. I examined two key players involved in the development of mammalian endochondral bones, which are also expressed in the regeneration of intramembranous bones of fin rays in zebrafish. I analyzed the expression and the function of *pthrp1* and *ihha* in the regeneration of bones in the caudal fins of zebrafish. The comparative studies between endochondral bone and intramembranous bone provide information that can have implication in helping us expand our understanding of bone diseases in humans using a new efficient model system. Some of these diseases, such as osteoporosis and osteoarthritis, affect a very large proportion of the population. Osteoporosis affects about 55% of Americans aged 50 and above (National Osteoporosis Foundation, 2002) and osteoarthritis of the knee affects approximately 250 million people worldwide (3.6% of the population) (Vos, 2012).

The roles of IHH and PTHrP have been described as essential in the development of the endochondral skeleton (Vortkamp et al., 1996, St-Jacques *et al.*, 1999, Kobayashi et al., 2002, Kronenberg 2006 and Mackie et al., 2008). The genome duplication event in teleosts, including zebrafish, has left them with two co-orthologs of the mammalian PTHrP. The Pthrp1 co-ortholog shows more similarity to the mammalian PTHrP than Pthrp2, which is why zebrafish *pthrp1* was the focus of this analysis. Expression of *pthrp1* showed that it is restricted to a distinct group of cells in the blastema of regenerating fin rays. This expression pattern is interesting because

although the bones of the caudal fin exoskeleton develop by intramembranous ossification, they are expressing chondrogenic markers like *pthrp1* and *ihha* during regeneration. This expression pattern is similar to the expression of *PTHrP* in the growth plate of endochondral bones in mammals. This led to my first hypothesis, which suggested that the expression pattern of *pthrp1* in regenerating fins hints at a possible role in the regeneration of bones similar to that in the growth plate. In mammalian endochondral ossification, the round proliferating chondrocytes are responsible for the release of PTHrP to act on all nearby chondrocytes expressing the common *PTH*/*PTHrP* receptor. The actions of PTHrP will keep the cells in the cell cycle to promote their proliferation. In newly regenerating fins, keeping cells in the cell cycle and proliferating is essential to keep the bone actively growing to replace the lost tissues. It is possible that during bone regeneration, Pthrp1 plays a similar role as it does in the mammalian growth plate in promoting proliferation and preventing differentiation. Since fin rays are intramembranous bone, the Pthrp1-expressing cells are not chondrocytes and they are not mature osteoblasts, rather they seem to be chondrocyte-like osteoblast cells expressing both chondrogenic and osteogenic factors. Previously Abzhanov and colleagues described a similar type of cells in the intramembranous bones of the craniofacial skeleton of chick and mice (Abzhanov et al., 2007). These cells, which are most likely osteoblast precursors, continue to release Pthrp1 to maintain the pool in constant proliferation. The cells begin to secrete Ihha when they eventually escape the zone of proliferation, and begin to differentiate to mature osteoblasts leading to the deposition of bone. Based on analysis of separate images of *in situ* hybridization, the expression domain of *pthrp1* seems to be in a subset of the cells that express *ihha* (Avaron et al., 2006), which means that the effects of Pthrp1 and Ihha are most likely exerted on the same cells. This provides further support to the possible interactive role played by Pthrp1 and Ihha in the regeneration of lepidotrichia possibly in a similar fashion to the

feedback loop seen in the mammalian growth plate. However, to have a better understanding of the spatial-temporal distribution of cells expressing *pthrp1* and *ihha,* it would be necessary to perform a double *in situ* hybridization of *pthrp1* and *ihha* probes. Unfortunately, the *ihha* probe did not give any signal during *in situ* hybridization experiments despite performing several trials. The reason behind this failure is unknown, since the probe has worked fine before with Avaron and colleagues.

To understand the spatial-temporal distribution of the effects exerted by Pthrp1 during regeneration of caudal fin bones, the expression of *pthrp1* receptors (*pth1r, pth2r* and *pth3r*) was analyzed using RT-PCR and *in situ* hybridization. RT-PCR analysis showed that the three receptors are expressed in both embryos at 4dpf and fin regenerates at 4dpa. However, their expression could not be detected by *in situ* hybridization. Hence, their detection by RT-PCR shows that the Pthrp1 ligand has a receptor to act upon in the regenerating fins. It would have been useful for my proposed idea to see expression patterns using *in situ* hybridization, especially for receptors in the fin regenerates, because it would give us an idea about the region of Pthrp1 influence. The released peptide must be acting on cells that express the receptor in the fin regenerates, which most likely is either pth1r or pth3r, because pth2r does not seem to be activated by zebrafish and human PTHrP (Rubin et al., 1999). Thus, in the future, performing the *in situ* on sections of fin regenerates would be a better alternative to achieve better probe penetration (Smith et al, 2008).

In addition to the expression pattern, morpholino knockdown analysis showed further evidence suggesting that Pthrp1 and Ihha play a role similar to their role in the mammalian growth plate. Three batches of fish were injected in the fin rays of dorsal lobe only with morpholinos for *pthrp1, ihha* or the standard control. At 2dpi, measurements the area of regenerative outgrowth covered by the four outer rays showed a significant reduction in the growth of the regenerate on

the morpholino-injected lobe versus the control lobe. This inhibition of growth indicates that Pthrp1 and Ihha have a role to play in the regeneration process because the knockdown of any one of these two factors resulted in a reduction in the growth of the regenerate. This result also supports the growth plate hypothesis suggesting that Pthrp1 could actually be involved in caudal fin regeneration as an important factor for proliferation by preventing cells from exiting the cell cycle. Therefore, the knockdown of *pthrp1* will result in reduced effects on the chondrocyte-like osteoblast cells expressing the receptors for Pthrp1, meaning less proliferation and rapid differentiation leading to reduced growth. In the case of *ihha*, if we expect the gene to act in a similar fashion to the mammalian Ihh, then it will have a positive effect on proliferation *via* Pthrp1. Therefore, we expected that the morpholino knockdown of *ihha* would result in reduced regenerative growth as well. The knockdown does support the hypothesis showing reduction in growth.

In an earlier assessment of the effects of morpholino knockdown, injections of morpholino were performed in both lobes of the fin (one lobe injected with the experimental morpholino and the other with the control morpholino) and the results the injections were analyzed at 4dpi. Measurements of the length of the outer four rays starting from the line of amputation did not show any significant difference in the fin ray length between the two lobes. One potential interpretation of the absence of effect is that the time point of observation for this assessment was too late and the morpholino injected fin rays managed to recover and catch up to the control fin ray length. Indeed the effects of morpholinos is transient. On the other hand, a few studies have shown that *pthrp1* and *ihha* mRNA have a rapid cycle rate. In a study on the half-life of the *PTHrP* mRNA in mammals, it has been reported that it is between 30 minutes and 3 hours (difference due to different isoforms) (Sellers et al., 2004). In another study on the half-life of *IHH* mRNA, it was reported

that it is about 4 hours (Murakami et al., 1997). The speed at which these fin rays managed to recover from the morpholino injection is still surprising. It is possible that there is compensatory roles provided by other genes of the *pthrp* or the *ihh* family such as *pthrp2* and *ihhb*. The phenomenon of compensation has been well described in the literature especially concerning genetic compensation by duplicated genes (Gu et al., 2003). In one study, it was shown that *ihha* zebrafish mutants had severe retardation in endochondral mineralization during embryogenesis, but all their bones did mineralize by 30dpf to the extent that they were indistinguishable from wild types. This is an indication that Ihha is crucial for the onset of endochondral mineralization, but the bones still managed to mineralize at a delayed time meaning that there is a possible partial redundancy between Ihha and Ihhb (Hammond & Schulte-Merker, 2009). However, Fabien did not detect *ihhb* expression in fin regenerates (Avaron et al, 2006). It is however possible that Shha may compensate for the absence of Ihha. This is especially true in zebrafish caudal fin regeneration because *shha* is expressed in the basal layer of the epidermis in a domain that is adjacent to that of *ihha* (Avaron et al., 2006). The Hh factors (Shh and Ihh) have been shown to have similar functions with functional redundancy in species like *Drosophila melanogaster* (Zhang et al., 2001). RT-PCR analysis shows that *pthrp2* is expressed in 4dpa fin regenerates, therefore, suggesting that it may potentially compensate for *pthrp1* loss of function. To examine this possibility in the fin regenerates, I need to confirm the spatial distribution of *pthrp2* by *in situ* hybridization. If I confirm that *pthrp2* is localized near *pthrp1* expression, then I can perform a double morpholino knockdown experiment (for example *pthrp1* and *pthrp2*) and compare the extent of regenerative outgrowth to that of a single knockdown (*pthrp1* morpholino only).

I also observed an expression at the level of already formed joints. It was not as pronounced as the expression pattern observed in the distal blastema, but it was visible on the joint edges. The presence of *pthrp1* at this domain leads towards my second hypothesis, which suggests that Pthrp1 plays a role in the formation and maintenance of joints of bone segments in the zebrafish fin rays. Previous expression analysis indicated that *evx1* is co-localized with *pthrp1*. Zebrafish that are *evx1* homozygous mutants have no joints in the fin rays of the caudal fin, which indicates that *evx1* is essential for joint formation. The co-localization of *evx1* and *pthrp1* provided another hint to a possible role of Pthrp1 in joints. The evx1 transcription factor may potentially regulate the expression of *pthrp1*. However, based on my RT-PCR, *pthrp1* is expressed in the regenerating fins of *evx1* homozygous mutants. However, this does not eliminate the possibility that Evx1 and Pthrp1 might be involved in different molecular pathways leading to joint formation.

The persistence of expression at already formed joints suggested that the role of Pthrp1 might be more than just being involved in the formation of joints. Studies have shown that mechanical loading on the joint of endochondral bone in mice induces the expression of PTHrP and the latter is required for continuous remodelling by recruitment of osteoblasts and osteoclasts (Chen et al., 2008). In zebrafish, and especially in the caudal fin, I speculate that there is continuous wear and tear on the joints due to the constant tail movement required for swimming. That makes maintenance of the anabolic/catabolic homeostasis at the level of the joints very important. This could explain a continuous role for Pthrp1 beyond the involvement in joint formation. This on-going need for Pthrp1 could be the reason behind the very faint expression at already formed joints compared to the typical expression at the level of the newly forming joint in the blastema. This faint expression can be explained based on the limitations of the *in situ* hybridization technique on whole-mount samples (Smith et al, 2008). At the level of already formed joints, the bone matrix is

fully formed and it is difficult for the probe to penetrate through. Alternatively, it is possible that the level of expression is determined by the need for Pthrp1. At the level of already formed joints, the need for Pthrp1 is limited only to the purpose of maintenance and minimal growth. At the level of the blastema, new joints must be formed and bones are in a rapid growth state with continuous proliferation and differentiation. Thus, the need for Pthrp1 is much higher. Therefore, the involvement of Pthrp1 in remodelling consists of anabolic/catabolic processes that possibly require it to be always active, but at a minimal level compared to the blastema of newly regenerating fins. I also observed the joints in the fin regenerates that have been injected with *pthrp1* morpholino, there was no morphological defects in the joints. This did not support my second hypothesis, but there could be unknown reasons for the absence of defect such as the possibility of compensation by Pthrp2.

Therefore, similar to the multiple roles PTHrP displayed in mammalian endochondral bone, *pthrp1* possibly plays multiple roles related to bones in the regenerating rays of the caudal fin. We have evidence that may support both of my hypotheses. First, the expression pattern of *pthrp1* and *ihha* plus the morpholino knockdown analysis indicates that there is a possible role played in regeneration and growth of bones. The roles of Pthrp1 and Ihha resembles the actions of mammalian PTHrP and IHH at the growth plate. In the second hypothesis, faint expression at the level of the joints in regenerating fin rays plus the co-localization of *pthrp1* with *evx1* by *in situ* hybridization, are indicators that Pthrp1 is possibly involved in joint formation and maintenance. It is possible that Pthrp1 and Ihha are involved in multiple roles in fin regeneration and this can only be confirmed by more experimentation and analysis at the level of expression and function.

4.1 Future directions

Therefore, in the future I would have to analyze the nature of the cells that are expressing *pthrp1* and *ihha*. It would be important to analyze the expression of different markers of osteoblasts maturation, such as *Runx2a*, which marks osteoblast at an early maturation stage. Another marker would be *osteocalcin*, which labels mature differentiated osteoblasts in the regenerate. The expression would be examined in *pthrp1* and *ihha* morpholino injected fins. The expression pattern of *runx2a* has been shown previously in differentiating osteoblasts in regenerating fins (Smith et al., 2006, Li et al., 2009 and Singh et al., 2012). Expression of *osteocalcin* has been described as well in fin regeneration in mature osteoblasts (Singh et al., 2012). These expression patterns are in the same area as *pthrp1* and according to the growth plate hypothesis, it is expected that the knockdown of *pthrp1* will perturb their expression pattern. In addition, it would be necessary for the support of my hypothesis that I determine the extent of proliferation in the regenerate following morpholino injections. This can be done by analyzing BrdU incorporation or PCNA immunodetection in proliferating cells, which allows me to determine the localization of proliferation along the regenerate at different time points. This proliferation analysis would be performed on both wild type fins and in morpholino injected fins. In the future, it would also be interesting to make fluorescence reporter transgenic lines for *pthrp1*. Reporter transgenic lines express the fluorescent protein (such as GFP) under the regulatory elements of the gene of interest and allow *in vivo* tracking of the dynamics of expression in embryos and also in the relatively transparent adult zebrafish fin. Another option is to design transgenic lines to ablate cells that express *pthrp1* or *ihha*. One way this can be done is by the metronidazole nitroreductase system, which is based on the ability of nitroreductase to convert the non-toxic pro-drug metronidazole into a cytotoxic agent, causing cell death (Bridge-water *et al.*, 1997). Hence, zebrafish can be used

as a tool to complement genetic and embryological studies in mammalian organisms to help clarify the molecular mechanisms underlying bone development and disease. In addition, zebrafish is ideally suited and a great model system to allow visualization of chondrocytes and osteoblasts *in vivo* over time.

5. References

Abbink W and Flik G. 2007. Minireview: parathyroid hormone-related protein in teleost fish. General and Comparative Endocrinology 152, 243–251.

Abzhanov A, Rodda SJ, McMahon AP, Tabin CJ. 2007. Regulation of skeletogenic differentiation in cranial dermal bone. Development 134, 3133-3144.

Akimenko MA, Mari-Beffa M, Becerra J, Geraudie J. 2003. Old questions, new tools, and some answers to the mystery of fin regeneration. Developmental dynamics 226, 190-201.

Avaron F, Hoffman L, Guay D, Akimenko MA. 2006. Characterization of two new zebrafish members of the hedgehog family: atypical expression of a zebrafish indian hedgehog gene in skeletal elements of both endochondral and dermal origins. Developmental dynamics 235, 478-489.

Aza-Blanc P, Lin HY, Ruiz I, Altaba A, Kornberg TB. 2000. Expression of the vertebrate Gli proteins in Drosophila reveals a distribution of activator and repressor activities. Development 127, 4293-4301.

Azevedo A. S., Grotek B., Jacinto A., Weidinger G., Saude L. 2011. The Regenerative capacity of the zebrafish caudal fin is not affected by repeated amputations. Plos One 6(7), e22820.

Borday V., Thaeron C., Avaron F., Brulfert A., Casane D., Laurenti P., Geraudie J. 2001. evx1 transcription in bony fin rays segment boundaries leads to a reiterated pattern during zebrafish fin development and regeneration. Developmental dynamics 220:91–98.

Bridgewater JA, Knox RJ, Pitts JD, Collins MK, Springer CJ. 1997. The bystander effect of the nitroreductase/CB1954 enzyme/prodrug system is due to a cell-permeable metabolite. Human Gene Therapy 10: 709-717.

Brittijn SA, Duivesteijn SJ, Belmamoune M, Bertens LF, Bitter W, de Bruijn JD, Champagne DL, Cuppen E, Flik G, Vandenbroucke-Grauls CM, Janssen RA, de Jong IM, de Kloet ER, Kros

A, Meijer AH, Metz JR, van der Sar AM, Schaaf MJ, Schulte-Merker S, Spaink HP, Tak PP, Verbeek FJ, Vervoordeldonk MJ, Vonk FJ, Witte F, Yuan H, Richardson MK. 2009. Zebrafish development and regeneration: new tools for biomedical research. The International Journal of Developmental Biology 53:835-850.

Chen X., Macica C. M., Nasiri A., Broadus A. E. 2008. Regulation of articular chondrocyte proliferation and differentiation by indian hedgehog and parathyroid hormone–related protein in mice. Arthritis & Rheumatism, Vol. 58, No. 12, 3788–3797.

Chen X, Macica C, Nasiri A, Judex S, Broadus AE. 2007. Mechanical regulation of PTHrP expression in entheses. Bone. 41(5):752-9.

Cubbage C. C. and Mabee P. M. 1996. Development of the cranium and paired fins in the zebrafish Danio rerio (Ostariophysi, Cyprinidae). Journal of Morphology 229:121-160.

De Papp A.E., Stewart A.F. 1993. Parathyroid hormone-related protein- a peptide of diverse physiological functions. Trends in Endocrinology & Metabolism 4, 181–187.

Echelard Y, Epstein DJ, St-Jacques B, Shen L, Mohler J, McMahon JA, McMahon AP. 1993. Sonic hedgehog, a member of a family of putative signaling molecules, is implicated in the regulation of CNS polarity. Cell 75:1417-1430.

Franz-Odendaal T. 2011. Induction and patterning of intramembranous bone. Frontiers in Bioscience 16:2734-46.

Franz-Odendaal T., Hall B. K., Witten P. E. 2006. Buried Alive: How Osteoblasts Become Osteocytes. Developmental dynamics 235, 176–190.

Gensure R, Ponugoti B, Gunes Y, Papasani M, Lanske B, Bastepe M, Rubin D, Juppner H. 2004. Identification and characterization of two parathyroid hormone-like molecules in zebrafish. Endocrinology 145, 1634–1639.

Gerber, H. P. and Ferrara, N. 2000. Angiogenesis and bone growth. Trends in Cardiovascular Medicine 10, 223-228.

Gu Z., Steinmetz M., Gu X., Scharfe C., Davis R. W., Li W. H. 2003. Role of duplicate genes in genetic robustness against null mutations. Nature 421: 63–66.

Hammond C. L. and Schulte-Merker S. 2009. Two populations of endochondral osteoblasts with differential sensitivity to Hedgehog signaling. Development 136, 3991-4000.

Han M, Yang X, Farrington JE, Muneoka K. 2003. Digit regeneration is regulated by Msx1 and BMP4 in fetal mice. Development 130, 5123-5132.

Han M, Yang X, Taylor G, Burdsal CA, Anderson RA, Muneoka K. 2005. Limb regeneration in higher vertebrates: developing a roadmap. The Anatomical Record Part B: The New Anatomist 287, 14-24.

Ho L, Alman B. Protecting the hedgerow: p53 and hedgehog pathway interactions. Cell Cycle 9, 506-511.

Huang P., A. Xiao, M. Zhou, Z. Zhu, S. Lin and B. Zhang. 2011. Heritable gene targeting in zebrafish using customized TALENs. Nature Biotechnology 29 (8), 699–700.

Hynes M, Stone DM, Dowd M, Pitts-Meek S, Goddard A, Gurney A, Rosenthal A. 1997. Control of cell pattern in the neural tube by the zinc finger transcription factor and oncogene Gli-1. Neuron 19, 15-26.

Ingham PW, McMahon AP. 2001. Hedgehog signaling in animal development: paradigms and principles. Genes and Development 15:3059-3087.

Iwamoto M, Kitagaki J, Tamamura Y, Gentili C, Koyama E, Enomoto H, Komori T, Pacifici M, Enomoto-Iwamoto M. 2003. Runx2 expression and action in chondrocytes are regulated by retinoid signaling and parathyroid hormone-related peptide (PTHrP). Osteoarthritis and Cartilage 11, 6–15.

Jopling C, Sleep E, Raya M, Martí M, Raya A, Izpisúa Belmonte JC. 2010. Zebrafish heart regeneration occurs by cardiomyocyte dedifferentiation and proliferation. Nature 464 (7288), 606-9.

Juppner H., Abou-Samra A., Freeman M., Kong X., Schipani E., Richards J., Kolakowski Jr. L., Hock J., Potts Jr. J., Kronenberg H. 1991. A G protein-linked receptor for parathyroid hormone and parathyroid hormone-related peptide. Science 254, 1024–1026.

Jung D., Oh E., Park S., Chang Y., Kim C., Choic S., Williams D. R. 2012. A novel zebrafish human tumor xenograft model validated for anti-cancer drug screening. Molecular BioSystems 8, 1930-1939.

Karaplis A. C., Luz A., Glowacki J., Bronson R. T., Tybulewicz V. L., Kronenberg H. M., Mulligan R. C. 1994. Lethal skeletal dysplasia from targeted disruption of the parathyroid hormone-related peptide gene. Genes and Development 8, 277-289.

Karp S. J., Schipani E., St-Jacques B., Hunzelman J., Kronenberg H., McMahon A. P. 2000. Indian Hedgehog coordinates endochondral bone growth and morphogenesis via Parathyroid Hormone related-Protein-dependent and independent pathways. Development 127, 543-548.

Knopf F., Hammond C., Chekuru A., Kurth T., Hans S., Weber C. W., Mahatma G., Fisher S., Brand M., Schulte-Merker S., Weidinger G. 2011. Bone Regenerates via Dedifferentiation of Osteoblasts in the Zebrafish Fin. Developmental Cell 20 (5), 713-724.

Kobayashi T., Chung U., Schipani E., Starbuck M., Karsenty G., Katagiri T., Goad D. L., Lanske B., Kronenberg H. M. 2002. PTHrP and Indian hedgehog control differentiation of growth plate chondrocytes at multiple steps. Development 129, 2977-2986.

Kos R, Reedy MV, Johnson RL, Erickson CA. 2001. The winged-helix transcription factor FoxD3 is important for establishing the neural crest lineage and repressing melanogenesis in avian embryos. Development 128: 1467–1479.

Kronenberg HM. 2006. PTHrP and skeletal development. Annals of the New York Academy of Sciences 1068, 1-13.

Laforest L, Brown CW, Poleo G, Geraudie J, Tada M, Ekker M, Akimenko MA. 1998. Involvement of the sonic hedgehog, patched 1 and bmp2 genes in patterning of the zebrafish dermal fin rays. Development 125:4175-4184.

Lagerstrom M, Hellstrom A, Gloriam D, Larsson T, Schioth H, Fredriksson R. 2006. The G protein-coupled receptor subset of the chicken genome. PLoS Computational Biology 2, e54.

Lanske B., Kraplis A. C., Lee K., Luz A., Vortkamp A., Pirro A., Karperien M., Defize L. H., Ho C., Mulligan R. C., Abou-Samra AB, Jüppner H, Segre GV, Kronenberg HM . 1996. PTH/PTHrP receptor in early development and Indian hedgehog-regulated bone growth. Science 273, 663-666.

Lenton K, James AW, Manu A, Brugmann SA, Birker D, Nelson ER, Leucht P, Helms JA, Longaker MT. 2011. Indian hedgehog positively regulates calvarial ossification and modulates bone morphogenetic protein signaling. Genesis 49 (10), 784-96.

Li N., Felber K., Elks P., Croucher P., Roehl H. H. 2009. Tracking gene expression during zebrafish osteoblast differentiation. Developmental dynamics 238, 459–466.

Long F., Chung U., Ohba S., McMahon J., Kronenberg H. M., McMahon A. P. 2004. Ihh signaling is directly required for the osteoblast lineage in the endochondral skeleton. Development 131, 1309-1318.

Lu C., Wan Y., Cao J., Zhu X., Yu J., Zhou R., Yao Y., Zhang L., Zhao H., Li H., Zhao J., He L., Ma G., Yang X., Yao Z., Guo X. 2013. Wnt-mediated reciprocal regulation between cartilage and bone development during endochondral ossification. Bone 53, 566–574.

Mackie EJ, Ahmed YA, Tatarczuch L, Chen KS, Mirams M. 2008. Endochondral ossification: how cartilage is converted into bone in the developing skeleton. The International Journal of Biochemistry & Cell Biology 40, 46-62.

Mackie E J, Tatarczuch L, Mirams M. 2011. The skeleton: a multi-functional complex organ. The growth plate chondrocyte and endochondral ossification. Journal of Endocrinology 211, 109–121.

Minina E., Kreschel C., Naski M. C., Ornitz D. M., Vortkamp A. 2002. Interaction of FGF, Ihh/Pthlh, and BMP Signaling Integrates Chondrocyte Proliferation and Hypertrophic Differentiation. Developmental Cell 3 (3), 439–449.

Morgan TH. 1901. Regeneration and Liability to Injury. Science 14, 235-248.

Moseley J.M., Kubota M., Diefenbach-Jagger H., Wettenhall R.E.H., Kemp B.E., Suva L.J., Rodda C.P., Ebeling P.R., Hudson P.J., Zajac J.D., Martin T.J. 1987. Parathyroid hormone-related protein purified from a human lung cancer cell line. Proceedings of the National Academy of Sciences 84, 5048–5052.

Murakami S., Nifuji A., Noda M. 1997. Expression of indian hedgehog in osteoblasts and its post-transcriptional regulation by transforming growth factor-β. Endocrinology Vol. 138, No. 5, 1972-1978.

National Osteoporosis Foundation. 2002. America's Bone Health: The State of Osteoporosis and Low Bone Mass in Our Nation. Washington, DC: National Osteoporosis Foundation.

Nechiporuk A. and Keating M.T. 2002. A proliferation gradient between proximal and msxb expressing distal blastema directs zebrafish fin regeneration. Development 129, 2607–2617.

Nguyen M and Karaplis A. 1998. The nucleus: a target site for parathyroid hormone-related peptide (PTHrP) action. Journal of Cellular Biochemistry 70, 193–199.

Nusslein-Volhard C and Wieschaus E. 1980. Mutations affecting segment number and polarity in Drosophila. Nature 287, 795-801.

Poleo G, Brown CW, Laforest L, Akimenko MA. 2001. Cell proliferation and movement during early fin regeneration in zebrafish. Developmental Dynamics 221, 380-390.

Poss KD, Keating MT, Nechiporuk A. 2003. Tales of regeneration in zebrafish. Developmental Dynamics 226, 202-210.

Poss K. D., Nechiporuk A., Hillam A. M., Johnson S. L. Keating M. T. 2002. Mps1 defines a proximal blastemal proliferative compartment essential for zebrafish fin regeneration. Development 129, 5141-5149.

Poss K.D., Shen J., Nechiporuk A., McMahon G., Thisse B., Thisse C., Keating M.T. 2000. Roles for Fgf signaling during zebrafish fin regeneration. Developmental Biology 222, 347–358.

Quint E., Smith A., Avaron F., Laforest L., Miles J., Gaffield W., Akimenko MA. 2002. Bone patterning is altered in the regenerating zebrafish caudal fin after ectopic expression of sonic hedgehog and bmp2b or exposure to cyclopamine. Proceedings of the National Academy of Sciences 99 (13), 8713-8718.

Rawls JF and Johnson SL. 2001. Requirements for the kit receptor tyrosine kinase during regeneration of zebrafish fin melanocytes. Development 128, 1943–1949.

Reginelli AD, Wang YQ, Sassoon D, Muneoka K. 1995. Digit tip regeneration correlates with regions of Msx1 (Hox 7) expression in fetal and newborn mice. Development 121, 1065-1076.

Rubin D.A., Hellman P., Zon L.I., Lobb C.J., Bergwitz C., Juppner H. 1999. A G protein-coupled receptor from zebrafish is activated by human parathyroid hormone and not by human or teleost parathyroid hormone-related peptide. The journal of Biological Chemistry. 274, 23035–23042.

Sasaki H, Nishizaki Y, Hui C, Nakafuku M, Kondoh H. 1999. Regulation of Gli2 and Gli3 activities by an amino-terminal repression domain: implication of Gli2 and Gli3 as primary mediators of Shh signaling. Development 126, 3915-3924.

Schebesta M., Lien C., Engel F. B., Keating M. T. 2006. Transcriptional Profiling of Caudal Fin Regeneration in Zebrafish. The Scientific World Journal 6(S1), 38-54.

Schulte J. Claus, Allen C., England S. J., Juarez-Morales J. L., Lewis K. E. 2011. Evx1 is required for joint formation in zebrafish Fin dermoskeleton. Developmental dynamics 240:1240–1248.

Sellers R. S., Luchin A. I., Richard V., Brena R. M., Lima D., Rosol T. J. 2004. Alternative splicing of parathyroid hormone-related protein mRNA: expression and stability. Journal of Molecular Endocrinology 33, 227–241.

Shao J., Qian X., Zhang C., Xu Z. 2009. Fin regeneration from tail segment with musculature, endoskeleton, and scales. Journal of Experimental Zoology Part B: Molecular and Developmental Evolution 312, 762-769.

Singh S. P., Holdway J. E., Poss K. D. 2012. Regeneration of amputated zebrafish fin rays from de novo osteoblasts. Developmental Cell. 22(4), 879–886.

Smith A., Avaron F., Guay D., Padhi B.K., Akimenko M.A. 2006. Inhibition of BMP signaling during zebrafish fin regeneration disrupts fin growth and scleroblast differentiation and function. Developmental Biology 299, 438–454.

Smith A, Zhang J, Guay D, Quint E, Johnson A, Akimenko MA. 2008. Gene expression analysis on sections of zebrafish regenerating fins reveals limitations in the whole-mount in situ hybridization method. Developmental Dynamics 237(2), 417-25.

Spoorendonk K. M., Hammond C. L., Huitema L. F. A., Vanoevelen J., Schulte-Merker S. 2010. Zebrafish as a unique model system in bone research: the power of genetics and in vivo imaging. Journal of Applied Ichthyology 26, 219–224.

Stainier, D.Y. 2001. Zebrafish genetics and vertebrate heart formation. Nature Reviews Genetics 2(1), 39–48.

Stewart S. and Stankunas K. 2012. Limited Dedifferentiation Provides Replacement Tissue during Zebrafish Fin Regeneration. Developmental Biology 365(2), 339–349.

St-Jacques B, Hammerschmidt M, McMahon AP. 1999. Indian hedgehog signaling regulates proliferation and differentiation of chondrocytes and is essential for bone formation. Genes and Development 13, 2072-2086.

Suda N, Kitahara Y, Hammond V.E, Ohyamaa K. 2003. Development of a novel mouse osteoclast culture system including cells of mandibular body and erupting teeth. Bone 33(1), 38–45.

Tal T. L., Franzosa J. A., Tanguay R. L. 2010. Molecular Signaling Networks That Choreograph Epimorphic Fin Regeneration in Zebrafish – A Mini-Review. Gerontology. 56(2), 231–240.

Thummel R., Bai S., Sarras M. P., Song Jr, P., McDermott J., Brewer J., Perry M., Zhang X., Hyde D. R., Godwin A. R. 2006. Inhibition of zebrafish fin regeneration using in vivo electroporation of morpholinos against fgfr1 and msxb. Developmental Dynamics 235(2), 336–346.

Tryon R. C. and Johnson S. L. 2012. Clonal and Lineage Analysis of Melanocyte Stem Cells and Their Progeny in the Zebrafish. Methods in Molecular Biology 916, 181–195.

Tu S. and Chi NC. 2012. Zebrafish models in cardiac development and congenital heart birth defects. Differentiation 84, 4–16.

Vidal P and Dickson MG. 1993. Regeneration of the distal phalanx. A case report. Journal of Hand Surgery British volume 18, 230-233.

Vortkamp A, Lee K, Lanske B, Segre GV, Kronenberg HM, Tabin CJ. 1996. Regulation of rate of cartilage differentiation by Indian hedgehog and PTH-related protein. Science 273, 613-622.

Vos, T. 2012. Years lived with disability (YLDs) for 1160 sequelae of 289 diseases and injuries 1990-2010: a systematic analysis for the Global Burden of Disease Study 2010. Lancet 380 (9859), 2163–96.

Wang M., VanHouten J. N, Nasiri A. R, Johnson R. L, Broadus A. E. 2013. PTHrP Regulates the Modeling of Cortical Bone Surfaces at Fibrous Insertion Sites During Growth. Journal of Bone and Mineral Research 28(3) 598–607.

Westerfield M. 1995. The zebrafish Book. University of Oregon Press.

Wienholds E, van Eeden F, Kosters M, Mudde J, Plasterk RH, Cuppen E. 2003. Efficient target-selected mutagenesis in zebrafish. Genome Research 13(12), 2700–2707.

Wysolmerski J.J., Philbrick W.M., Dunbar M.E., Lanske B., Kronenberg H., Broadus A.E. 1998. Rescue of the parathyroid hormone-related protein knockout mouse demonstrates that parathyroid hormone-related protein is essential for mammary gland development. Development 125, 1285-1294.

Yan Y., Bhattacharya P., Jun He X., Ponugoti B., Marquardt B., Layman J., Grunloh M., Postlethwait J. H, Rubin D. A. 2012. Duplicated zebrafish co-orthologs of parathyroid hormone-related peptide (PTHrP, Pthlh) play different roles in craniofacial skeletogenesis. Journal of Endocrinology 214, 421-435.

Yokoyama H. 2008. Initiation of limb regeneration: the critical steps for regenerative capacity. Development Growth and Differentiation 50, 13-22.

Zhang XM, Ramalho-Santos M, McMahon AP. 2001. Smoothened mutants reveal redundant roles for Shh and Ihh signaling including regulation of L/R symmetry by the mouse node. Cell. 106(2), 781-92.

Zhang J, Wagh P, Guay D, Sanchez-Pulido L, Padhi BK, Korzh V, Andrade-Navarro MA, Akimenko MA. 2010. Loss of fish actinotrichia proteins and the fin-to-limb transition. Nature 466, 234-237.